

Unification of BL Lac objects, FR I and FR II(G) radio galaxies and Doppler factor Estimation for BL Lac Objects

Xu-Hong YE^{1,2,3} and Jun-Hui FAN^{1,2,3}

¹Center for Astrophysics, Guangzhou University, Guangzhou 510006, China

²Astronomy Science and Technology Research Laboratory of Department of Education of Guangdong Province, Guangzhou 510006, China

³Key Laboratory for Astronomical Observation and Technology of Guangzhou, Guangzhou 510006, China

*E-mail: fjh@gzhu.edu.cn

Received 2020 July 30; Accepted 2021 April 19

Abstract

In this work, we collected a sample of BL Lacs, FR I and FR II(G) radio galaxies with available core and extended emissions from published works to discuss the unified schemes and estimate the Doppler factor for BL Lacs. Wilcoxon rank-sum test and Kolmogorov-Smirnov test both suggest that the probabilities for the distribution of the extended luminosity of BL Lacs and that of FR I and FR II(G) radio galaxies to be from the same parent distribution are $p_{\text{WRS}} = 0.779$ and $p_{\text{K-S}} = 0.326$, suggesting they are unified. Based on this unified schemes, we propose to estimate the Doppler factors for BL Lacs. Comparing the Doppler factor estimated by the fitting/regression method with those for the common sources in the literatures, we found a good linear correlation for common sources.

Key words: Active galactic nuclei (AGNs)- Galaxies: Active-Galaxies: BL Lacs-Galaxies: Jets

1 Introduction

Active Galactic Nuclei (AGNs) are a special class of galaxies, showing extreme observation properties. Blazars are the extreme class of AGNs, which can be subdivided into two subclasses because of their behavior of emission lines: BL Lacertae objects (BL Lacs) with weak or no emission line and flat-spectrum radio quasars (FSRQs) with strong ones. BL Lacs show some extreme observation properties such as rapid and high amplitude variation, high and variable polarization, very weak or no emission line features, superluminal motions, or even high energy γ -ray emissions (Stickel et al. 1991; Fan et al. 1999; Fan et al. 2002; Xiao et al. 2019). When the viewing angle between relativistic jet and line of sight is small, a Doppler beaming effect should be taken into considered. The observed flux density

S^{ob} is enhanced by the Doppler factor, $S^{\text{ob}} = S^{\text{in}} \delta^q$, where S^{in} is the intrinsic flux density, and δ is a Doppler factor, $q = 2 + \alpha$ for a continuous jet, $q = 3 + \alpha$ for a spherical jet (Scheuer & Readhead 1979), in which α is the spectral index ($S_\nu \propto \nu^{-\alpha}$, S_ν for the monochromatic flux density). The Doppler factor is important for emissions in BL Lacs, which is determined by velocity (β) and the viewing angle (θ): $\delta = [\Gamma(1 - \beta \cos \theta)]^{-1}$, where Γ is the Lorentz factor, satisfying $\Gamma = 1/\sqrt{1 - \beta^2}$.

Some methods were proposed to estimate the Doppler factor (Ghisellini et al. 1993; Mattox et al. 1993; Lähtemäki & Valtaoja 1999; Fan et al. 2013; Chen 2018; Lioudakis et al. 2018; Zhang et al. 2020). Ghisellini et al. (1993) adopted the synchrotron self-Compton (SSC) model and assumed the synchrotron high frequency cut-off as 10^{14} Hz to obtain the Doppler factors. Their re-

sults show that the Doppler factors are the largest for core-dominated quasars, intermediate for BL Lacs, and the smallest for radio galaxies and lobe-dominated quasars. Lähteemäki & Valtaoja (1999) adopted a method using the total radio flux density variations to assess Doppler factors and found high-polarization quasars with higher Doppler factors, while BL Lacs and low-polarization quasars have smaller Doppler factors. Following Mattox et al. (1993), Fan et al. (2013) assumed the γ -ray timescale as one day and calculated the lower limit for γ -ray Doppler factors from X-ray and γ -ray emissions. Based on the spectral energy distributions (SEDs) model, Chen (2018) estimated the Doppler factors for a sample of 999 blazars. The Doppler factor of BL Lacs is significantly larger than that of FSRQs in the work by Chen (2018). Liodakis et al. (2018) analyzed and constrained the average equipartition brightness temperature (T_{eq}) of the whole sample same as those ($T_{eq} = 2.78 \times 10^{11} K$) of FSRQs to obtain Doppler factors for a larger sample of blazars, showing that blazars are strongly beamed sources with higher Doppler factor on average than that of radio galaxies and unclassified sources. Zhang et al. (2020) proposed a new method based on the correlation between γ -ray luminosity and broad-line region luminosity to estimate the Doppler factors for a sample of 350 blazars. We can see that different method gives different Doppler factor value because of the different assumption in the literatures. For instance, based on the SSC model, Ghisellini et al. (1993) obtained a Doppler factor of $\delta = 2.1$ for the BL Lac 0716+714, while Hovatta et al. (2009) obtained $\delta = 10.9$ using the radio variation and Liodakis et al. (2018) derived a Doppler factor $\delta = 31.3$ by adopting the same intrinsic brightness temperature for all the samples.

Radio galaxies are also a subclass of AGNs. From a work by Fanaroff & Riley (1974), the radio galaxies are classified into two types, based on their luminosity and the morphology. For some sources, the radio luminosity is mainly from the central part, this radio galaxy is classified as class I, called as Fanaroff-Riley class I (FR I) radio galaxy; some sources that their radio luminosity is mainly from the outer edge of the galaxy, this type of radio galaxy is regarded as class II radio galaxies, and called as Fanaroff-Riley class II (FR II) radio galaxy (Fanaroff & Riley 1974). The central compact core emission in FR I radio galaxies (hereafter FR Is) is found to be identified with strongly associated with optical synchrotron radiation, which is produced in the inner regions of the relativistic jet (Chiaberge et al. 1999). In addition, Verdoes et al. (2002) had analyzed a complete sample of 21 nearby FR Is and proposed that the radio and optical core emissions of these samples are likely synchrotron radiation from inner jet because (a)

radio and optical core emission are closely correlated, (b) the radio to optical spectral indices are similar to those for extended optical jets, (c) there is a suggestive trend with independent estimates from jet orientation, (d) the residual for radio- $H\alpha$ + $[N II]$ core correlation and that for optical- $H\alpha$ + $[N II]$ core correlation are well correlated with each other. From the optical spectrum, FR II radio galaxy can be subdivided into two subclass: FR II(G) and FR II(Q). The FR II(G) radio galaxy shows its optical type as that of a galaxy, while the spectral type of FR II(Q) resemble an optical type of a quasar (Xie et al. 1993).

In the unification of AGNs, the viewing angle is invoked to explain the different observation properties of AGNs. It was proposed that BL Lacs and FR Is were unified, in this unified scheme, the FR Is are the parent population of the BL Lacs (Urry et al. 1991; Ghisellini et al. 1993; Urry & Padovani 1995). Urry et al. (1991) discussed the unification of BL Lacs and FR Is by computing luminosity functions, and found this samples were consistent with the beaming hypothesis that the BL Lacs are FR Is seen face on. Ghisellini et al. (1993) computed the average Lorentz factor ($\Gamma = 8.32$) and viewing angle ($\theta = 11.8$) for a sample of BL Lacs, which are consistent with other results from the attempts to unify FR I/BL Lac schemes, suggesting that the FR Is should be the parent population of the BL Lacs. Meanwhile, some authors suggested that FR II radio galaxies may be a part of parent population for BL Lacs (Xie et al. 1993; Owen et al. 1996; Fan et al. 1997). Xie et al. (1993) discussed the unified schemes of 75 BL Lacs, 27 FR I and 45 FR II(G) radio galaxies (hereafter FR II(G)s) using the Hubble diagram, and found BL Lacs and FR Is and FR II(G)s fit the same Hubble relation very well, supporting the unified schemes of BL Lacs and FR Is should include the FR II(G)s.

Due to the unobservable characteristics, it is difficult to obtain the Doppler factor. The previous studies mentioned above used different hypothesis to assess the Doppler factor (Ghisellini et al. 1993; Mattox et al. 1993; Lähteemäki & Valtaoja 1999; Fan et al. 2013; Chen 2018; Liodakis et al. 2018; Zhang et al. 2020). In this sense, any method estimating the Doppler factor is important for AGN studying. In a two-component model (Urry & Shafer 1984), the core with a relativistic jet plus extended component is considered, in which the core emission is enhanced by the Doppler beaming effect, while the extended component has no beaming effect and shows their intrinsic emission. Since the extended emissions are unbeamed, then we can discuss the relationship of the extended luminosity for BL Lacs and FR I with FR II(G) radio galaxies (hereafter FR I/II(G)s). If BL Lacs and FR I/II(G)s are unified with FR I/II(G)s being the parent population of

BL Lacs, then based on this unified schemes, we assumed that the intrinsic core and extended luminosity of BL Lacs should follow the same correlation as that of FR I/II(G)s, then we can estimate the Doppler factor of BL Lacs by using the core to extended luminosity fitting/regression method or ratio method of FR I/II(G)s. The structure of this work is arranged as follows. In Sect. 2, the unified schemes for BL Lacs and FR I/II(G)s is discussed using Wilcoxon rank-sum (WRS) test and Kolmogorov-Smirnov (K-S) test. In Sect. 3, based on this unified model, we estimate the Doppler factor. In Sect. 4, some discussions are presented, and some conclusions are shown in Sect. 5.

2 Samples and unified schemes

2.1 Samples

In this work, we collected 297 BL Lacs, 87 FR Is and 41 FR II(G)s with core and extended fluxes or luminosities at 5 GHz from the literature and showed them in Table 1, in which the core and extended fluxes at 5 GHz are listed in Col. 3-4 with their references in Col. 5, and their corresponding luminosities are listed in Col. 7-8. For some sources, their core and extended luminosities are available in the literatures (Zirbel & Baum 1995; Broderick & Fender 2011; Fan et al. 2011) as listed in Col. 7-9. Generally, the measured frequency of data is different in different literature. Because most of the measured radio frequency is at 5 GHz, Fan et al. (2011) and Pei et al. (2019) transferred the data at other measured frequency to 5 GHz, $S_c^{5GHz} = S_c^{\nu, obs}$, $S_{ext}^{5GHz} = S_{ext}^{\nu, obs} (\frac{\nu}{5GHz})^{\alpha_{ext}}$, with $\alpha_{ext} = 0.75$ and $\alpha_c = 0.0$ (Fan et al. 2011; Pei et al. 2019).

We compare BL Lacs in the present sample (BL Lacs_{TW}, 297 sources) with BL Lacs (BL Lacs_{ref}, 649 sources) in the references (Fan et al. 2011; Pei et al. 2019) and Roma-BZCAT (Massaro et al. 2015), to discuss the completeness of BL Lacs of the sample. The redshift of BL Lacs_{TW} is in the range of 0.026 to 3.2, and the coverage range for redshift distribution of BL Lacs_{TW} is similar to that of BL Lacs_{ref}, which is also in the range of 0.026 to 3.2, as shown in the upper panel of Fig. 1. Additionally, the fraction between BL Lacs_{TW} and BL Lacs_{ref} is obtained in different redshift bin and presented in the lower panel of Fig. 1. About half of BL Lacs_{ref} within redshift < 1 and almost all the BL Lacs_{ref} with redshift > 1 were selected for research. FR I/IIs in the present sample (FRs_{TW}, 128 sources) are also compared with FR I/IIs (FRs_{ref}, 395 sources) in the references (Mattox et al. 1993; Zirbel & Baum 1995; Broderick & Fender 2011; Fan et al. 2011; Pei et al. 2019). The redshift distribution of FRs_{TW} is in a range of 0.003 to 1.132, and that of FRs_{ref} ranges from

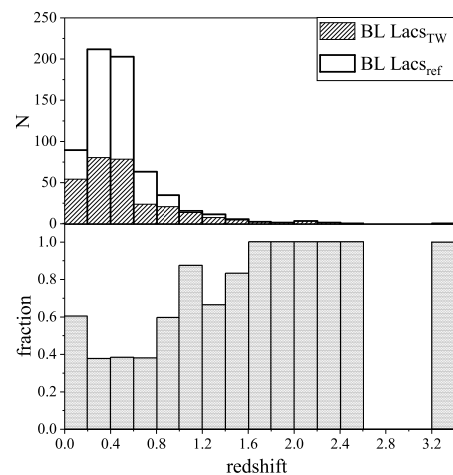


Fig. 1. The upper panel is the redshift distributions for BL Lacs, the un-hatched area for BL Lacs (BL Lacs_{ref}) in the references (Fan et al. 2011; Pei et al. 2019) and Roma-BZCAT (Massaro et al. 2015), the hatching area for BL Lacs in the present sample (BL Lacs_{TW}). The lower panel is the fraction between BL Lacs_{TW} and BL Lacs_{ref} in different redshift bin.

0.002 to 2.009, as shown in upper panel of Fig. 2. The fraction between FRs_{TW} and FRs_{ref} in different redshift bin is also presented in the lower panel of Fig. 2. One can see that the present sample has a smaller redshift than that from the references. We think that the reason is because the radio galaxy with higher redshift is weak so that it is hard for one to obtain the core and the extended emissions, therefore we can only separate the core and the extended emissions for the low redshift radio galaxy. We hope that we can obtain more core and extended emissions with higher redshift in the future.

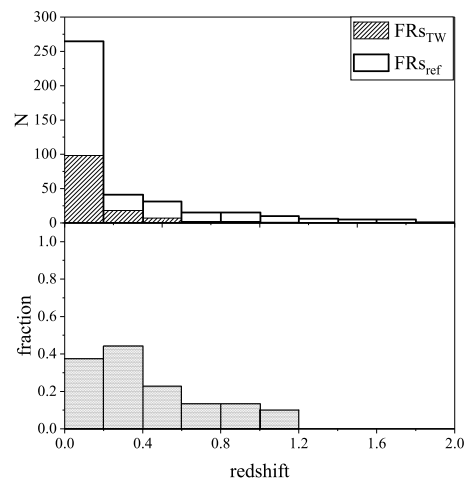


Fig. 2. The upper panel is the redshift distributions for FR I/II, the un-hatched area for FR I/II (FRs_{ref}) in the references (Mattox et al. 1993; Zirbel & Baum 1995; Broderick & Fender 2011; Fan et al. 2011; Pei et al. 2019), the hatching area for FR I/II in the present sample (FRs_{TW}). The lower panel is the fraction between FRs_{TW} and FRs_{ref} in different redshift bin.

Table 1. The core and extended fluxes or luminosities of whole samples and the Doppler factor of BL Lacs.

Source Name	class	z	S_{core} (mJy)	S_{ext} (mJy)	Ref	$\log L_{\text{core}}$ (W Hz $^{-1}$)	$\log L_{\text{ext}}$ (W Hz $^{-1}$)	Ref	δ_2 ($\alpha_c = 0$)	δ_2 (0.5)	δ_2 (-0.5)	δ_3 ($\alpha_c = 0$)	δ_3 (0.5)	δ_3 (-0.5)
(1)	(2)	(3)	(4)	(5)	(6)	(7)	(8)	(9)	(10)	(11)	(12)	(13)	(14)	(15)
0003+003	B	1.037	480	206	P19	27.17	26.81		18.74	10.43	49.79	7.06	5.34	10.43
0003-066	B	0.347	1850	1504.47	P19	26.73	26.64		12.55	7.57	29.16	5.40	4.24	7.57
0007+124	I	0.156	4	751.02	F11	23.47	25.75							
0007+472	B	0.280	67	22	P19	25.17	24.69		7.69	5.11	15.17	3.90	3.21	5.11
0011+1853	B	0.473	140	104	P19	25.89	25.76		8.58	5.58	17.57	4.19	3.42	5.58
0013+790	II(G)	0.840	4.4	1028.6	F11	25.21	27.58							
0021+055	B	2.050	28	53	P19	26.56	26.83		9.04	5.82	18.84	4.34	3.52	5.82
0029-271	B	0.333	11	105	P19	24.67	25.65		2.27	1.93	2.98	1.73	1.60	1.93
0032+595	B	0.086	44	5	P19	23.92	22.97		5.71	4.03	10.20	3.19	2.71	4.03
0033+156	B	1.162	125	28	P19	26.96	26.31		20.43	11.18	55.86	7.47	5.61	11.18
0038+328	II(G)	0.482	0.47	1199.53	NED	23.64	27.05							
0039+398	I	0.109	1	225	P19	22.52	24.88							
0043+008	B	2.149	2	2	P19	25.27	25.27		5.86	4.11	10.55	3.25	2.75	4.11
0044+193	B	0.181	7	17	P19	23.71	24.10		2.13	1.83	2.74	1.65	1.54	1.83
0048-09	B	0.634	887	108.45	F11	26.98	26.07		24.62	12.97	71.62	8.46	6.24	12.97
0052+251	B	0.154	1	1	P19	22.73	22.73		1.71	1.54	2.05	1.43	1.36	1.54
0053+260	I	0.195				23.00	25.04	F11						
...

Note: Col. 1 gives the source name, Col. 2 the classification, B for BL Lacs, I for FR I, II(G) for FR II(G), Col. 3 redshift, Col. 4 the core flux density at 5 GHz, Col. 5 the extended flux density at 5 GHz, Col. 6 the references for Col. 4 and 5, NED for NASA/IPAC Extragalactic Database, M93 for Morganti et al. (1993), PS93 for Perlman & Stocke (1993), K05 for Kovalev et al. (2005), K10 for Kharb et al. (2010), F11 for Fan et al. (2011), DM14 for Di Mauro et al. (2014), P19 for Pei et al. (2019), Col. 7 the core luminosity at 5 GHz, Col. 8 the extended luminosity at 5 GHz, Col.9 the references for Col. 7 and 8, Z95 for Zirbel & Baum (1995), B11 for Broderick & Fender (2011), Col. 10 the Doppler factor for $q = 2$, $\alpha_c = 0$, Col. 11 the Doppler factor for $q=2$, $\alpha_c = 0.5$, Col. 12 the Doppler factor for $q = 2$, $\alpha_c = -0.5$, Col. 13 the Doppler factor for $q = 3$, $\alpha_c = 0$, Col. 14 the Doppler factor for $q = 3$, $\alpha_c = 0.5$, Col. 15 the Doppler factor for $q = 3$, $\alpha_c = -0.5$. (A portion is shown here for guidance regarding its form and content. The Table 1 is published in its entirety in Appendix.)

2.2 Luminosity Calculation

From the core and extended fluxes, one can calculate the corresponding luminosities, $L = 4\pi d_L^2 S_\nu$, where d_L is a luminosity distance expressed by

$$d_L = (1+z) \frac{c}{H_0} \int_1^{1+z} \frac{1}{\sqrt{\Omega_M x^3 + 1 - \Omega_M}} dx \quad (1)$$

with $\Omega_\Lambda \sim 0.692$, $\Omega_M \sim 0.308$ and $H_0 = 67.8 \text{ km s}^{-1} \text{ Mpc}^{-1}$ (Planck Collaboration et al. 2016).

For the 297 BL Lacs, our calculation shows that the logarithm of the core luminosity, $\log L_{\text{core}}$, is in a range of $\log L_{\text{core}} = 21.96 \text{ -- } 28.70$ with an average of 25.53, where L_{core} indicates the core luminosity in the unit of W Hz $^{-1}$, and that of the extended luminosity, $\log L_{\text{ext}}$, is in a range of $\log L_{\text{ext}} = 21.56 \text{ -- } 28.19$, where L_{ext} indicates the extended luminosity in the unit of W Hz $^{-1}$.

For the 87 FR Is, we have $\log L_{\text{core}} = 20.90 \text{ -- } 25.40$ with an average of 23.32 for the core luminosity, and $\log L_{\text{ext}} = 22.49 \text{ -- } 26.80$ with an average of 24.43 for the extended luminosity. While for the 41 FR II(G)s, the core luminosity is found to be in a range from $\log L_{\text{core}} =$

22.69 -- 26.56 with an average of 24.43 and the extended luminosity in a range of $\log L_{\text{ext}} = 25.14 \text{ -- } 27.85$ with an average of 26.35.

2.3 Unification Scheme

From the relativistic two-component model (Urry & Shafer 1984), the total luminosity consists of the core (beamed) luminosity and extended (unbeamed) luminosity, in which core luminosity is enhanced by the relativistic beaming effect, while the extended luminosity displays its intrinsic value. In order to investigate the unification between BL Lacs and FR I/II(G)s, we used the extended luminosity for these samples. Because of the FR I/FR II dichotomy from the Fanaroff & Riley (1974), the different property in the luminosity between the FR I and FR II is widely accepted for decades. FR Is show their behavior as low radio power, and FR IIs behave as high radio power owing to their different jet effect. In our samples, the FR II(G)s have a higher extended luminosity ranging from $\log L_{\text{ext}} = 25.14 \text{ -- } 27.85$, but FR Is have lower extended luminosity,

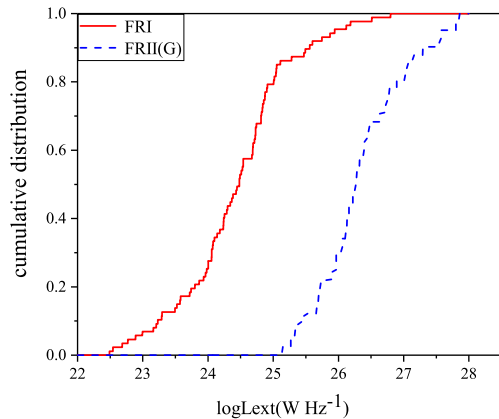


Fig. 3. The cumulative distributions for extended luminosity of FR Is and FR II(G)s, in which the solid line represents FR Is and broken line represents FR II(G)s.

$\log L_{\text{ext}} = 22.46 \text{ -- } 26.80$. The cumulative distributions for extended luminosity of FR Is and FR II(G)s are presented in Fig. 3.

As for BL Lacs and FR Is, the extended luminosity distribution of BL Lacs ($\log L_{\text{ext}} = 21.56 \text{ -- } 28.19$) is wider than that of FR Is ($\log L_{\text{ext}} = 22.49 \text{ -- } 26.80$) and BL Lacs have a higher average extended luminosity than that of FR Is. There is a marginal difference for low luminosity of BL Lacs and FR Is, but clear difference for high luminosity as shown in the left panel of Fig. 4, the probability values for the K-S test and WRS test are both $< 10^{-4}$, in which the hypothesis for WRS test as did Lioudakis et al. (2018) is to determine whether the two independent samples are from the same distribution and for K-S test is to discriminate between two statistical distributions, their p value threshold is taken as 0.05.

The extended luminosities for BL Lacs and FR II(G)s are also discussed. The extended luminosities for FR II(G)s are almost the high luminosity ($\log L_{\text{ext}} = 25.14 \text{ -- } 27.85$), so the cumulative distribution for extended luminosity of BL Lacs renders discrepant result from that of FR II(G)s with both $p < 10^{-4}$ for K-S test and WRS test as shown in right panel of Fig. 4.

It is proposed that the FR Is and FR II(G)s are the parent population of BL Lacs as we mentioned above (Xie et al. 1993; Owen et al. 1996; Fan et al. 1997). If it is the case, one can expect that, for the extended luminosity, the distribution of FR I/II(G)s and that of BL Lacs should be from the same parent distribution. Now, we will investigate those distributions using WRS test and K-S test. For the FR I/II(G)s, the total extended luminosity is in a range of $\log L_{\text{ext}} = 22.49 \text{ -- } 27.85$ with an average value 25.04, and their cumulative distribution for extended

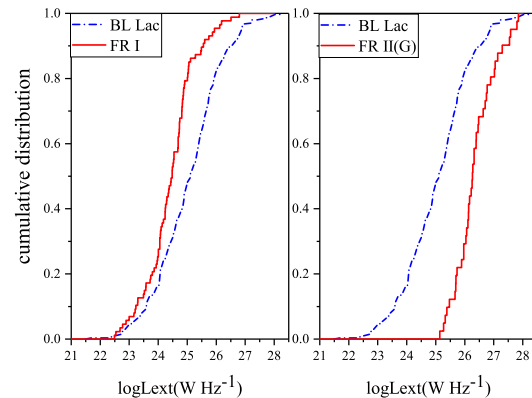


Fig. 4. The left panel is the cumulative distributions for extended luminosity of BL Lacs and FR Is, in which the solid line represents FR Is and broken-dotted line represents BL Lacs. The right panel is the cumulative distributions for extended luminosity of BL Lacs and FR II(G)s, in which the solid line represents FR II(G)s and broken-dotted line represents BL Lacs.

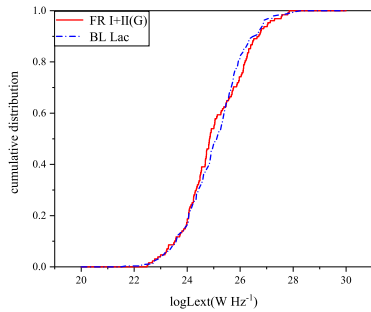
luminosity is close to that of BL Lacs, in which the corresponding cumulative distributions for extended luminosity of BL Lacs and FR I/II(G)s are shown in Fig. 5(a). When the WRS test and K-S test are adopted to the distribution of extended luminosity of BL Lacs and that of FR I/II(G)s, it is found that the probabilities for the both extended luminosities to be from the same parent distribution are $p_{\text{WRS}} = 0.779$ and $p_{\text{K-S}} = 0.326$, implying that the null hypothesis cannot be reject, suggesting that the extended luminosity distribution for BL Lacs and that of FR I/II(G)s are from the same parent distribution, which indicates that the BL Lacs and FR I/II(G)s are unified.

We also compared the core luminosity for BL Lacs and FR I/II(G)s. The total core luminosity for FR I/II(G)s is spanning from $\log L_{\text{core}} = 20.90$ to 26.56 with an average of 23.67, while the core luminosity for BL Lac is from $\log L_{\text{core}} = 21.96$ to 28.70 with an average of 25.53. The core luminosity distribution for FR I/II(G)s is significantly different from that of BL Lacs as presented in Fig. 5(b). Both the WRS test and K-S test give $p < 10^{-4}$, showing that the core luminosity of BL Lacs and that of FR I/II(G)s are from different distributions. The discrepancy for core luminosity between BL Lacs and FR I/II(G)s is due to the strong beaming effect in BL Lacs.

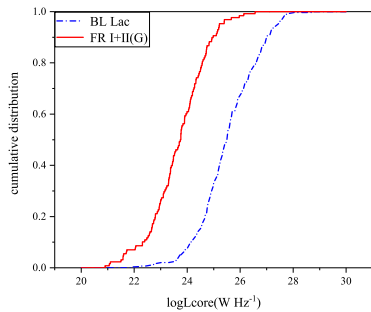
3 Estimation of Doppler Factor

3.1 Methodology

When the jet direction of a BL Lac is close to our line of sight, it causes a strong beaming effect for the core emission, $S_{\text{core}}^{\text{ob}} = \delta^q S_{\text{core}}^{\text{in}}$, where $S_{\text{core}}^{\text{ob}}$ and $S_{\text{core}}^{\text{in}}$ are the observed core flux density and the intrinsic core flux density



(a)



(b)

Fig. 5. The cumulative distributions of BL Lacs and FR I/II(G)s: (a) for extended luminosity. (b) for core luminosity. The solid line represents the FR I/II(G)s, and the broken-dotted line represents the BL Lacs.

of BL Lacs, $q = 2 + \alpha_c$ or $3 + \alpha_c$ from different jet structure (Scheuer & Readhead 1979), and α_c is the radio core spectral index of BL Lacs ($S_{\text{core},\nu} \propto \nu^{-\alpha_c}$). For luminosities, one can get $L_{\text{BL,core}}^{\text{ob}} = \delta^q L_{\text{BL,core}}^{\text{in}}$, in which the $L_{\text{BL,core}}^{\text{ob}}$ and $L_{\text{BL,core}}^{\text{in}}$ are the observed core luminosity and intrinsic core luminosity of BL Lacs.

As we mentioned in §2.3, BL Lacs and FR I/II(G)s are unified. In this sense, one can expect that the intrinsic luminosity of BL Lacs and that of FR I/II(G)s should be from the same parent population, and that the intrinsic luminosity of BL Lacs and that of FR I/II(G)s should follow the same correlation. Both core luminosity and extended luminosity depend on redshift, and a significant linear correlation ($\log L_{\text{ext}} = 1.18 \log L_{\text{core}} - 4.8$) between core and extended luminosity for radio galaxies is shown in Kollgaard et al. (1996). So, we assume that there is a linear correlation between core luminosity ($L_{\text{FR,core}}$) and extended luminosity ($L_{\text{FR,ext}}$) for FR I/II(G)s

$$\log L_{\text{FR,core}} = k \log L_{\text{FR,ext}} + b. \quad (2)$$

where k and b are the slope and intercept for FR I/II(G)s. It is clear that the intrinsic luminosity in FR I/II(G)s are almost the same as the observed luminosity since the

beaming effect is very weak. While for BL Lacs, one has observed core luminosity enhanced by Doppler factor, $L_{\text{BL,core}}^{\text{ob}} = \delta^q L_{\text{BL,core}}^{\text{in}}$, and extended luminosity shows as intrinsic luminosity. From unification of BL Lacs and FR I/II(G)s, the intrinsic core luminosity ($L_{\text{BL,core}}^{\text{in}}$) and extended luminosity ($L_{\text{BL,ext}}$) for BL Lacs should follow the same correlation as do FR I/II(G)s, namely $\log L_{\text{BL,core}}^{\text{in}} = k \log L_{\text{BL,ext}} + b$. So, we can get the Doppler factor, δ , for BL Lacs,

$$\log \delta = (\log L_{\text{BL,core}}^{\text{ob}} - k \log L_{\text{BL,ext}} - b)/q \quad (3)$$

3.2 Luminosity Correlation

The relation between the core and extended luminosity is shown in Figure 6 (a) and (b) for the BL Lacs and FR I/II(G)s, respectively.

The correlation coefficient $r = 0.678$ and $p < 10^{-4}$ are obtained between the core and extended luminosities of BL Lacs. When a linear regression is adopted to BL Lacs, we found that.

$$\log L_{\text{BL,core}}^{\text{ob}} = (0.67 \pm 0.04) \log L_{\text{BL,ext}} + 8.86 \pm 1.05 \quad (4)$$

As for FR I/II(G)s, the $r = 0.656$ and $p < 10^{-4}$ are obtained between the core and extended luminosities. When a linear regression is performed to the core and extended luminosities of FR I/II(G)s, we obtained following correlation.

$$\log L_{\text{FR,core}} = (0.58 \pm 0.06) \log L_{\text{FR,ext}} + 9.08 \pm 1.51 \quad (5)$$

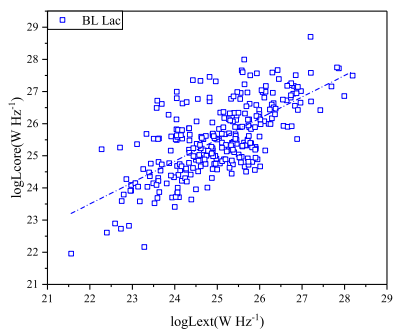
The best fitting results are shown in Figure 6 (a), (b). It is shown that there are moderate correlations between core and extended luminosities for both BL Lacs and FR I/II(G)s respectively. Since the differences in the slope and intercept between BL Lacs and FR I/II(G)s are smaller than three times the fitting error, the slope and intercept of BL Lacs are consistent to those of FR I/II(G)s within the fitting errors.

3.3 Doppler Factor

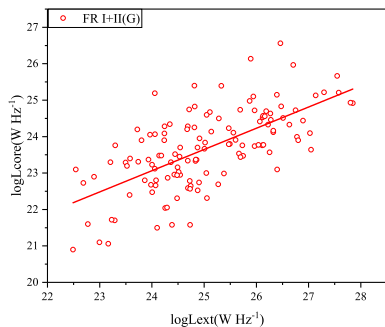
In the unified model, FR I/II(G)s are the parent population of BL Lacs. It means that BL Lacs are the FR radio galaxies with the jets pointing to the observers and boosted. As mentioned in §3.1, one can get an expression for a Doppler factor based on the slope k (0.58), intercept b (9.08) for the linear correlation of FR I/II(G)s,

$$\log \delta = (\log L_{\text{BL,core}}^{\text{ob}} - 0.58 \log L_{\text{BL,ext}} - 9.08)/q \quad (6)$$

When radio core spectral index $\alpha_c = 0.0$ (Donate et al. 2001; Abdo et al. 2010; Fan et al. 2016) is adopted, Doppler factors are obtained in a range from $\delta = 0.62$ to 113.08 with



(a)



(b)

Fig. 6. Distributions of core and extended luminosity: (a) for BL Lacs, the broken-dotted line represents the best linear regression between core and extended luminosity for BL Lacs. (b) for FR I/II(G)s, the solid line represents the best linear regression between core and extended luminosity for FR I/II(G)s.

an average of 15.03 for $q = 2$, and from $\delta = 0.73$ to 23.38 with an average of 5.43 for $q = 3$, which are listed in Col. 2-3 in Table 2. The Doppler factors from different literatures for BL Lacs are also presented in Table 2.

In addition, based on the unification of BL Lacs and FR I/II(G)s, we propose another method about the core to extended emission ratio of FR I/II(G)s to estimate Doppler factor. The core to extended emission ratio is also called as core-dominance parameter (R), using the expression, $R = S_{\text{core}}/S_{\text{ext}}$, or $R = L_{\text{core}}/L_{\text{ext}}$. If the core emission is strongly boosted by beaming effect, a close relation between the core-dominance parameter (R) and Doppler factor (δ) should be expected, which have been proposed by Ghisellini et al. (1993): $R = f\delta^q$, where the $f = S_{\text{core}}^{\text{in}}/S_{\text{ext}}$, $q = 2 + \alpha_c$ or $3 + \alpha_c$ (see above). When an unification of BL Lacs, FR Is and FR II(G)s is considered, the intrinsic core to extended emission ratio (f_{BL}) of BL Lacs should behave as the same as those (R_{FR}) of FR I/II(G)s, then a Doppler factor can be estimated from following correlation.

$$\delta^q = R_{\text{BL}}/R_{\text{FR}} \quad (7)$$

where R_{FR} is the core-dominance parameter ($R_{\text{FR}} = L_{\text{FR,core}}/L_{\text{FR,ext}}$) for the FR I/II(G)s, and R_{BL} is the observed core-dominance parameter ($R_{\text{BL}} = L_{\text{BL,core}}^{\text{ob}}/L_{\text{BL,ext}}$) for the BL Lacs. The density distributions of logarithm of core-dominance parameter of BL Lacs and FR I/II(G)s are shown in Figure 7. For the present FR I/II(G)s sample, they shows a peak at $\log R_{\text{FR}} = -1.48$ in Figure 7. When we used this value to estimate the Doppler factors for the case of $q = 2 + \alpha_c$ and $3 + \alpha_c$, the Doppler factor values are listed in Col. 4 and Col. 5 in Table 2.

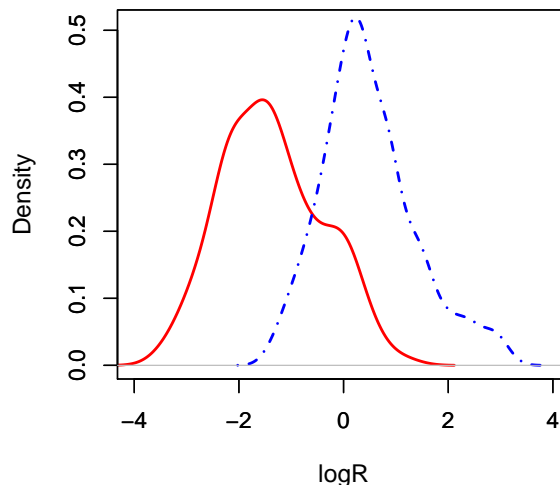


Fig. 7. The density distributions of logarithm of core-dominance parameter of BL Lacs and FR I/II(G)s. The broken-dotted line represents BL Lacs and the solid line represents FR I/II(G)s.

Table 2. δ from methods and different literatures for BL Lacs

	$q=2^{\dagger}$	$q=3^{\dagger}$	$q=2^{\ddagger}$	$q=3^{\ddagger}$	G93	H09	L18	Z20
(1)	(2)	(3)	(4)	(5)	(6)	(7)	(8)	(9)
Min	0.62	0.73	1.15	1.10	0.01	1.1	0.22	0.35
Max	113.08	23.38	201.01	34.32	14.3	24	60.36	53.57
Medium	8.25	4.08	8.24	5.93	2.1	6.3	9.78	7.09
Mean	15.03	5.43	18.23	4.08	3.85	7.9	13.03	10.32

\dagger The Doppler factor estimation by the core to extended fitting/regression method.

\ddagger The Doppler factor estimation by the core to extended flux ratio method.

Note: Col. 1 is parameters of samples, Col. 2 Doppler factor at $q = 2$ by fitting/regression method, Col. 3 Doppler factor at $q = 3$ by fitting/regression method, Col. 4 Doppler factor at $q = 2$ by ratio method, Col. 5 Doppler factor at $q = 3$ by ratio method, Col. 6 Doppler factor by Ghisellini et al. (1993), Col. 7 Doppler factor by Hovatta et al. (2009), Col. 8 Doppler factor by Lioudakis et al. (2018), Col. 9 Doppler factor by Zhang et al. (2020).

From different assumptions and methods, it can be

found that some Doppler factors for BL Lacs are smaller than unity, which may be caused by the systematic error or the limitation of the methods. For examples, there are 8 BL Lacs in Ghisellini et al. (1993), 5 BL Lacs in Liodakis et al. (2018), and 3 BL Lacs in Zhang et al. (2020) with Doppler factor $\delta < 1$. Liodakis et al. (2018) adopted a definite intrinsic brightness temperature to estimate the Doppler factor for BL Lacs. If some BL Lacs was in a low state when it was observed, it is possible to obtain a low observed brightness temperature, then to derive a Doppler factor $\delta < 1$ from the limitation of the methods. In our sample, the source 1440+356 with Doppler factor $\delta < 1$ in fitting/regression method may also be due to our systematic error or the limitation of our method that the unification of BL Lacs and FR I/II(G)s.

4 Discussions

BL Lacs show special observation properties, such as variability, high and variable polarization, high luminosity, high energetic γ -ray emissions, or superluminal motion etc. Their special observation properties are due to the beaming effect. When their jets are perpendicular to the line of sight, they are radio galaxies, and FR Is and FR II(G)s are proposed to be the parent population of BL Lacs (Xie et al. 1993; Owen et al. 1996; Fan et al. 1997).

From the available extended luminosities of BL Lacs and FR I/II(G)s, we can see that the probabilities from WRS test and K-S test render discrepant results, $p = 0.779$ for WRS test and $p = 0.326$ for K-S test. These results suggest, for the case of the extended luminosity, that BL Lacs are unified with FR I/II(G)s. But there is also a different probability by the WRS test and K-S test, which may be due to the difference in extended luminosity distributions of BL Lacs and FR I/II(G)s. The extended luminosity distribution of BL Lacs is similar to a normal distribution, but that of FR I/II(G)s is marginally different to normal distribution, in particular from $\log L_{\text{ext}} = 25$ to 26 shown in Fig. 8. The asymptotic relative efficiency of the WRS test compared to the t -test is 0.955 for normal distributions, indicating that it can be effectively used for both normal and nonnormal situations (Feigelson & Babu 2012), while K-S test is not. So the marginal difference of extended luminosity distributions between BL Lacs and FR I/II(G)s is represented in probability that the p value (0.779) for WRS test is higher than that (0.326) of K-S test.

However, the averaged value of the core luminosity of BL Lacs is higher than that of FR I/II(G)s, both WRS test and K-S test suggest that the probabilities for the distribution of the logarithm of the core luminosities of FR I/II(G)s and that of BL Lacs to come from the same parent

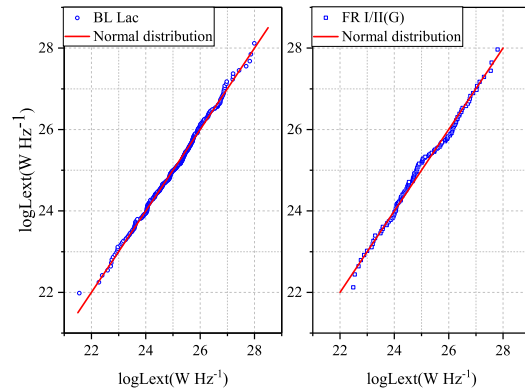


Fig. 8. The left panel is the comparison between the extended luminosity distribution of BL Lacs and normal distribution, in which the solid line represents normal distribution and the circular represents BL Lacs. The right panel is the comparison between the extended luminosity distribution of FR I/II(G)s and normal distribution, in which the solid line represents normal distribution and the square represents FR I/II(G)s.

distribution are very low, they are both $p < 10^{-4}$. The clear difference is from the fact that the core luminosities of BL Lacs are strongly beamed.

As mentioned in §1, many methods were proposed to estimate the Doppler factors (Ghisellini et al. 1993; Mattox et al. 1993; Lähteemäki & Valtaoja 1999; Fan et al. 2013; Chen 2018; Liodakis et al. 2018; Zhang et al. 2020). In the present work, based on the unified scheme of BL Lacs and FR I/II(G)s, the Doppler factor of BL Lacs is estimated. For BL Lacs objects, the radio band spectrum is flat. For example, Fan et al. (2006) obtained the radio average value of radio spectral index to be 0.235 for X-ray selected BL Lacs, and 0.044 for radio selected BL Lacs. Pei et al. (2016) studied a samples of 1335 blazars and showed the average radio spectral index, $\langle \alpha_{\text{radio}} \rangle = 0.02 \pm 0.31$ for *Fermi*-detected BL Lacs, 0.34 ± 0.37 for non-*Fermi*-detected BL Lacs. $-0.5 \leq \alpha \leq 0.5$ was adopted for BL Lacs in Yuan (2014). $\alpha_c = 0.0$ was also adopted for BL Lacs by Donate et al. (2001); Abdo et al. (2010), and Fan et al. (2016). We adopted the radio core spectral index $\alpha_c = 0.0$ for the radio spectral index. By comparing the Doppler factor between $\alpha_c = 0$ and $\alpha_c = \pm 0.5$, we can find that the Doppler factor for the case $\alpha_c = \pm 0.5$ could be several times different from that of $\alpha_c = 0$ for $q = 2$. But for $q = 3$, there is marginal difference between $\alpha_c = \pm 0.5$ and $\alpha_c = 0$ to estimate the Doppler factor. The Doppler factor corresponding $\alpha_c = 0$ or ± 0.5 are listed in Col. 10-15 in Table 1.

The coefficients of regression lines have some degrees of errors as shown in Equations (4) and (5). When we estimated the Doppler factor using the fitting/regression method, the coefficient errors of regression lines do have a great influence, even on the order of magnitude, on the

Doppler factor value, but the average fitting/regression should be representative of the true Doppler factor values.

Following the case of the spherical jet ($q=3$) (Ghisellini et al. 1993; Xie et al. 1993; Hovatta et al. 2009; Liodakis et al. 2018) and the radio core spectral index as 0 (Donate et al. 2001; Abdo et al. 2010; Fan et al. 2016), we can also compare our Doppler factor estimation results (δ_{TW}) with those (δ_{G} by Ghisellini et al. (1993), δ_{H} by Hovatta et al. (2009), δ_{L} by Liodakis et al. (2018), δ_{Z} by Zhang et al. (2020)) from the literatures for the common sources. There are 29 sources in common with Ghisellini et al. (1993), we performed a linear regression and obtained $\delta_{\text{TW}} = (0.78 \pm 0.13)\delta_{\text{G}} + 4.84 \pm 0.75$, with a Spearman's rank correlation coefficient of $r = 0.541$ and a chance probability of $p = 2.4 \times 10^{-3}$, see the upper-left panel in Figure 9. We also performed the regression for the common sources with Hovatta et al. (2009) $\delta_{\text{TW}} = (0.70 \pm 0.13)\delta_{\text{H}} + 4.39 \pm 1.10$, Liodakis et al. (2018) $\delta_{\text{TW}} = (0.17 \pm 0.05)\delta_{\text{L}} + 4.88 \pm 0.67$ and Zhang et al. (2020) $\delta_{\text{TW}} = (0.41 \pm 0.09)\delta_{\text{Z}} + 3.86 \pm 1.27$. The Spearman's rank correlation coefficients and chance probabilities are $r = 0.656$ and $p = 3 \times 10^{-3}$ for 18 sources with Hovatta et al. (2009); $r = 0.537$ and $p = 3 \times 10^{-4}$ for 41 sources with Liodakis et al. (2018), and $r = 0.537$ and $p = 0.016$ for 20 sources with Zhang et al. (2020). The best fitting results are all shown in Figure 9. The correlation coefficients for our Doppler factor estimation results with other literatures for common sources are both larger than 0.5 with probabilities < 0.05 , indicating that our Doppler factor estimation by fitting/regression method is correlated with other samples.

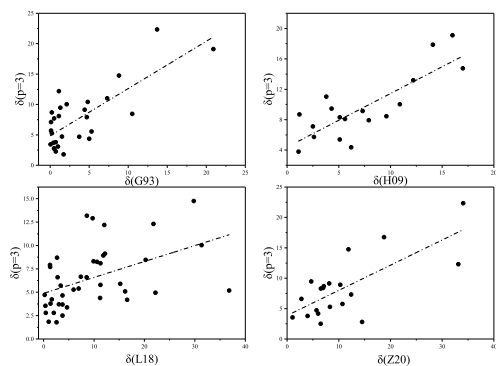


Fig. 9. Plot of the correlation for common sources between our Doppler factor (δ_{TW}) by the fitting/regression method and those from Ghisellini et al. (1993), δ_{G} , Hovatta et al. (2009), δ_{H} , Liodakis et al. (2018), δ_{L} , Zhang et al. (2020), δ_{Z} .

We also compare the correlations for common sources with other Doppler factor (δ_{G} , δ_{H} , δ_{L} , δ_{Z}) for Doppler factor ($q=3$) estimation of the core to extended flux ra-

tio method as do the core to extended luminosity fitting/regression method. The Spearman's rank correlation coefficients between the ratio method and those samples are $r = 0.347$ and $p = 0.07$ for Ghisellini et al. (1993), $r = 0.411$, $p = 0.09$ for Hovatta et al. (2009), $r = 0.182$, $p = 0.254$ for Liodakis et al. (2018), and $r = 0.513$, $p = 0.022$ for Zhang et al. (2020). A detailed comparison between the ratio method and fitting/regression method is listed in Table 3. From Table 3, a comparison of the distributions of the core to extended flux ratio is straightforward, but the correlation coefficients of this ratio method are less relevant and less convincing than those of fitting/regression method as mentioned above.

Table 3. A comparison between the fitting/regression method and the ratio method.

samples	r_f^\dagger	p_f^\dagger	r_r^\ddagger	p_r^\ddagger
(1)	(2)	(3)	(4)	(5)
G93	0.541	2.4×10^{-3}	0.347	0.07
H09	0.656	3×10^{-3}	0.411	0.09
L18	0.537	3×10^{-4}	0.182	0.254
Z20	0.537	0.016	0.513	0.022

† The correlation coefficients and probabilities for fitting/regression method.

‡ The correlation coefficients and probabilities for ratio method.

Note: Col. 1 are samples, Col. 2 the correlation coefficients for fitting/regression method, Col. 3 the probabilities for fitting/regression method, Col. 4 the correlation coefficients for ratio method, Col. 5 the probabilities for ratio method.

5 Conclusions

In this work, we compiled the core and extend flux densities for a sample of BL Lacs, FR Is and FR II(G)s, and calculated their corresponding luminosities. We used WRS test and K-S test to analyze the cumulative distribution for extended luminosity, L_{ext} , of BL Lacs and that of FR I/II(G)s, and found that the probabilities for the both to be from the same distribution are $p_{\text{WRS}} = 0.779$ and $p_{\text{K-S}} = 0.326$. Based on the unification of BL Lacs and FR I/II(G)s, we proposed a core to extended luminosities fitting/regression method and a ratio method of core to extended emissions to estimate the Doppler factor for BL Lacs, and compared our results with those in the literatures. Our conclusions are as follows:

1. From the extended radio luminosities, BL Lacs are unified with FR I and FR II(G) radio galaxies, which confirmed the results by Xie et al. (1993), Owen et al. (1996), Fan et al. (1997).

2. Our Doppler factors from the fitting/regression method is correlated with those by Ghisellini et al. (1993), Hovatta et al. (2009), Liodakis et al. (2018), and Zhang et

al. (2020).

3. The Doppler factors of BL Lacs estimated by the fitting/regression method is in a range of from $\delta = 0.73$ to $\delta = 23.38$ for the case of $q = 3$, $\alpha_c = 0$.

Acknowledgments

The work is supported by the National Natural Science Foundation of China (NSFC U2031201, NSFC 11733001, NSFC U1938110, NSFC U1531245), Natural Science Foundation of Guangdong Province (2019B030302001), Guangzhou University (NO YM2020001, No 2019GDJC-D18), and supports for Astrophysics Key Subjects of Guangdong Province and Guangzhou City. We thank the anonymous referee for the comments that made us improve our manuscript.

Appendix. The complete Table 1 sample.

References

- Abdo, A. A., et al. 2010, ApJ, 716, 30
- Best, P. N., & Heckman, T.M. 2012, MNRAS, 421, 1569
- Broderick, J. W., & Fender, R. P. 2011, MNRAS, 417, 184
- Capetti, A., Massaro, F., & Baldi, R. D. 2017, A&A, 598, A49
- Chen, L. 2018, ApJS, 235, 39
- Chiaberge, M., Capetti, A., & Celotti, A. 1999, A&A, 349, 77
- Donate, D., Ghisellini, G., Tagliaferri, G., & Fossati, G. 2001, A&A, 375, 739
- Di Mauro, M., Calore, F., Donato, F., Ajello, M., & Latronico, L. 2014, ApJ, 781, 161
- Fanaroff, B. L., & Riley, J. M. 1974, MNRAS, 167, 31P
- Fan, J. H., et al. 2006, PASJ, 58, 945
- Fan, J. H., & Lin, R. G. 1999, ApJS, 121, 131
- Fan, J. H., Lin, R. G., Xie, G. Z., Zhang, L., Mei, D. C., Su, C. Y., & Peng, Z. M. 2002, A&A, 381, 1
- Fan, J. H., Okudaira, A., Lin, R. G., & Xie, G. Z. 1997, Ap&SS, 167, 275
- Fan, J. H., et al. 2016, ApJ, 226, 20
- Fan, J. H., Yang, J. H., Liu, Y., & Zhang, J. Y. 2013, RAA, 13, 259
- Fan, J. H., Yang, J. H., Pan, J., & Hua, T. X. 2011, RAA, 11, 1413
- Feigelson, E. D., & Babu, G. J. 2012, Modern Statistical Methods for Astronomy With R Applications (the United Kingdom: Cambridge University Press), p. 113.
- Ghisellini, G., Padovani, P., Celotti, A., & Maraschi, L. 1993, ApJ, 407, 65
- Hovatta, T., Valtaoja, E., Tornikoski, M., & Lähteenmäki, A. 2009, A&A, 494, 527
- Kharb, P., Lister, M. L., & Cooper, N. J. 2010, ApJ, 710, 764
- Kovalev, Y. Y., et al. 2005, AJ, 130, 2473
- Kollgaard, R. I., Palma, C., Laurent-Muehleisen, S. A., & Feigelson, E. D. 1996, ApJ, 465, 115
- Lähteenmäki, A., & Valtaoja, E. 1999, ApJ, 521, 493
- Laing, R. A., Riley, J. M., & Longair, M. S. 1983, MNRAS, 204, 151
- Liodakis, I., Hovatta, T., Huppenkothen, D., Kiehlmann, S., Max-Moerbeck, W., & Readhead, A. C. S. 2018, ApJ, 866, 137
- Massaro, E., Maselli, A., Leto, C., Marchegiani, P., Perri, M., Giommi, P., & Piranomonte, S. 2015, Ap&SS, 351, 1
- Mattox, J. R., et al. 1993, ApJ, 410, 609
- Morganti, R., Killeen, N. E. B., & Tadhunter, C. N. 1993, MNRAS, 263, 1023
- Owen, F. N., Ledlow, M. J., & Keel, W. C. 1996, AJ, 111, 53
- Pei, Z. Y., Fan, J. H., Bastieri, D., Sawangwit, U., & Yang, J. H. 2019, RAA, 19, 70
- Pei, Z. Y., Fan, J. H., Liu, Y., Yuan, Y. H., Cai, W., Xiao, H. B., Lin, C., & Yang, J. H. 2016, Ap&SS, 361, 237
- Perlman, E. S., & Stocke, J. T. 1993, ApJ, 406, 430
- Planck Collaboration, Ade, P. A. R., et al. 2016, A&A, 594, A13
- Scheuer, P. A. G., & Readhead, A. C. S. 1979, Nature, 277, 18
- Stickel, M., Padovani, P., Urry, C. M., Fried, J. W., & Kühn, H. 1991, ApJ, 374, 431
- Urry, C. M., & Padovani, P. 1995, PASP, 107, 803
- Urry, C. M., Padovani, P., & Stickel, M. 1991, ApJ, 382, 501
- Urry, C. M., & Shafer, R. A. 1984, ApJ, 280, 569
- Verdoes, Kleijn, G. A., Baum, S. A., De, Zeeuw, P. T., & O'Dea, C. P. 2002, AJ, 123, 1334
- Xiao, H. B., et al. 2019, Sci. China-Phys. Mech. Astron, 62, 129811
- Xie, G. Z., Zhang, Y. H., Fan, J. H., & Liu, F. K. 1993, A&A, 278, 6
- Yang, J. H., Nie, J. J., & Fan, J. H. 2014, J. Astrophys. Astr., 35, 487
- Yuan, Y. H. 2014, J. Astrophys. Astr., 35, 417
- Zhang, L. X., Chen, S. N., Xiao, H. B., Cai, J. T., & Fan, J. H. 2020, ApJ, 897, 10
- Zirbel, E. L., & Baum, S. A. 1995, ApJ, 448, 521

Table 1. The core and extended fluxes or luminosities of whole samples and the Doppler factor of BL Lacs.

Source Name	class	z	S_{core} (mJy)	S_{ext} (mJy)	Ref	$\log L_{\text{core}}$ (W Hz^{-1})	$\log L_{\text{ext}}$ (W Hz^{-1})	Ref	δ_2 ($\alpha_c = 0$)	δ_2 (0.5)	δ_2 (-0.5)	δ_3 ($\alpha_c = 0$)	δ_3 (0.5)	δ_3 (-0.5)
(1)	(2)	(3)	(4)	(5)	(6)	(7)	(8)	(9)	(10)	(11)	(12)	(13)	(14)	(15)
0003+003	B	1.037	480	206	P19	27.17	26.81		18.74	10.43	49.79	7.06	5.34	10.43
0003-066	B	0.347	1850	1504.47	P19	26.73	26.64		12.55	7.57	29.16	5.40	4.24	7.57
0007+124	I	0.156	4	751.02	F11	23.47	25.75							
0007+472	B	0.280	67	22	P19	25.17	24.69		7.69	5.11	15.17	3.90	3.21	5.11
0011+1853	B	0.473	140	104	P19	25.89	25.76		8.58	5.58	17.57	4.19	3.42	5.58
0013+790	II(G)	0.840	4.4	1028.6	F11	25.21	27.58							
0021+055	B	2.050	28	53	P19	26.56	26.83		9.04	5.82	18.84	4.34	3.52	5.82
0029-271	B	0.333	11	105	P19	24.67	25.65		2.27	1.93	2.98	1.73	1.60	1.93
0032+595	B	0.086	44	5	P19	23.92	22.97		5.71	4.03	10.20	3.19	2.71	4.03
0033+156	B	1.162	125	28	P19	26.96	26.31		20.43	11.18	55.86	7.47	5.61	11.18
0038+328	II(G)	0.482	0.47	1199.53	NED	23.64	27.05							
0039+398	I	0.109	1	225	P19	22.52	24.88							
0043+008	B	2.149	2	2	P19	25.27	25.27		5.86	4.11	10.55	3.25	2.75	4.11
0044+193	B	0.181	7	17	P19	23.71	24.10		2.13	1.83	2.74	1.65	1.54	1.83
0048-09	B	0.634	887	108.45	F11	26.98	26.07		24.62	12.97	71.62	8.46	6.24	12.97
0052+251	B	0.154	1	1	P19	22.73	22.73		1.71	1.54	2.05	1.43	1.36	1.54
0053+260	I	0.195				23.00	25.04	F11						
0055-01	I	0.045	93	2043.47	M93	23.67	25.01							
0057+026	B	0.599	99	16	P19	25.83	25.04		13.02	7.80	30.65	5.54	4.34	7.80
0057+3021	I	0.017				23.40	23.58	B11						
0059+581	B	0.644	1570	7	P19	27.32	24.96		75.51	31.80	319.16	17.86	11.83	31.80
0104+32	I	0.016				22.04	24.25	Z95						
0106+130	II(G)	0.060	38	5140.8	F11	23.53	25.67							
0106+729	II(G)	0.181				23.76	26.11	F11						
0107+32224	I	0.017				22.80	23.86	B11						
0109+224	B	0.265	330	5.44	F11	25.82	24.04		25.12	13.18	73.56	8.58	6.31	13.18
0109+492	II(G)	0.395	3.64	734.59	NED	24.33	26.63							
0115-261	I	0.053	18	5	P19	23.10	22.54							
0118-272	B	0.559	1137	63	P19	26.97	25.71		30.74	15.49	96.28	9.81	7.08	15.49
0120+340	B	0.272	31	2	P19	24.81	23.62		10.35	6.48	22.55	4.75	3.80	6.48
0121+318	B	0.654	82	89	P19	26.08	26.11		8.42	5.50	17.14	4.14	3.38	5.50
0122+090	B	0.339	1	1	P19	23.52	23.52		2.51	2.09	3.41	1.85	1.69	2.09
0123+3315	I	0.016				20.90	22.49	B11						
0125+287	II(G)	0.437	185	105	NED	26.14	25.89							
0125-0120	I	0.018				22.80	24.08	B11						
0138-097	B	0.733	696	504	P19	26.93	26.79		14.33	8.42	34.82	5.90	4.58	8.42
0140+219B	B	0.599	7	13	P19	24.89	25.16		4.07	3.07	6.49	2.55	2.23	3.07
0145+138	B	0.125	2	1	P19	22.89	22.59		2.27	1.92	2.98	1.72	1.60	1.92
0154+286	II(G)	0.735	5.3	536.7	NED	25.13	27.14							
0156+0537	I	0.019				21.70	23.29	B11						
0158+003	B	0.299	9	1	P19	24.37	23.41		7.14	4.82	13.74	3.71	3.07	4.82
0159+002	B	0.163	7	12	P19	23.70	23.94		2.34	1.98	3.12	1.77	1.63	1.98
0200-0011	B	0.366	30	88	P19	25.04	25.51		3.82	2.92	5.98	2.45	2.15	2.92
0204+29	I	0.110	171	158	P19	24.75	24.71							
0208+352	B	0.318	5	1	P19	24.31	23.61		5.85	4.11	10.54	3.25	2.74	4.11
0208-512	B	0.999	233	3169	P19	26.86	27.99		5.91	4.14	10.69	3.27	2.76	4.14

Table 1. (Continued)

Source Name	class	z	S_{core} (mJy)	S_{ext} (mJy)	Ref	$\log L_{\text{core}}$ (W Hz $^{-1}$)	$\log L_{\text{ext}}$ (W Hz $^{-1}$)	Ref	δ_2 ($\alpha_c = 0$)	δ_2 0.5	δ_2 -0.5)	δ_3 ($\alpha_c = 0$)	δ_3 0.5	δ_3 -0.5)
(1)	(2)	(3)	(4)	(5)	(6)	(7)	(8)	(9)	(10)	(11)	(12)	(13)	(14)	(15)
0212+364	B	0.490	82	1	P19	25.54	23.63		23.91	12.67	68.86	8.30	6.13	12.67
0213-132	I	0.147	99	98	P19	24.82	24.82							
0214+083	B	1.400	296	166	P19	27.12	26.87		16.94	9.62	43.51	6.60	5.04	9.62
0219+042	I	0.022	161	130	P19	23.30	23.21							
0219+428	B	0.444	814	510.84	F11	26.75	26.55		13.67	8.10	32.68	5.72	4.46	8.10
0220+427	I	0.021				22.59	24.69	F11						
0221+27	II(G)	0.310	20	884	F11	24.83	26.48							
0227+020	B	0.457	9	18	P19	24.76	25.06		3.74	2.87	5.80	2.41	2.12	2.87
0230+344	B	0.458	123	56	P19	25.89	25.55		9.92	6.27	21.31	4.62	3.71	6.27
0232+202	B	0.599	43	7	P19	25.68	24.89		12.06	7.33	27.65	5.26	4.15	7.33
0232+264	B	0.599	554	1	P19	26.79	24.05		76.10	32.00	322.50	17.96	11.89	32.00
0240+1656	B	0.599	40	7	P19	25.65	24.89		11.63	7.12	26.35	5.13	4.06	7.12
0245+269A	B	0.599	28	1	P19	25.49	24.05		17.11	9.70	44.09	6.64	5.07	9.70
0247-027	I	0.087				23.45	24.53	Z95						
0255+05	I	0.024				22.65	24.74	Z95						
0257+342	B	0.245	9	2	P19	24.15	23.49		5.25	3.77	9.12	3.02	2.58	3.77
0300+162	I	0.033	8	1188.74	F11	22.31	24.48							
0300+470	B	0.475	1566	62.16	F11	26.95	25.55		33.63	16.65	108.56	10.42	7.45	16.65
0301-243	B	0.260	228	132	F11	25.67	25.43		8.30	5.44	16.81	4.10	3.35	5.44
03020-037	I	0.005	28	102	P19	23.37	23.93							
0305+03	I	0.029	964	2436	DM14	24.28	24.68							
0307+169	II(G)	0.256	6.04	963.14	F11	24.12	26.32							
0308+0406	I	0.029				24.20	24.67	B11						
0308+104	B	0.599	886	1	P19	26.99	24.05		96.24	38.61	441.05	21.00	13.59	38.61
0314+063	B	0.599	27	2	P19	25.48	24.35		13.74	8.14	32.91	5.74	4.47	8.14
0315+41	I	0.026	40	3490	P19	22.78	24.72							
0317+185	B	0.190	17	15	P19	24.22	24.17		3.65	2.82	5.62	2.37	2.10	2.82
0319+4130	I	0.018				25.40	24.81	B11						
0320-37	I	0.006	51	71949	DM14	21.58	24.73							
0329+704	B	0.599	37	12	P19	25.53	25.04		9.19	5.90	19.25	4.39	3.55	5.90
0331-001	I	0.139				24.53	26.12	Z95						
0350-371	B	0.165	14	2.9	P19	24.04	23.35		5.08	3.67	8.74	2.96	2.53	3.67
0356+102	I	0.030	9	4961	P19	22.31	25.05							
036-019	B	0.850	14	2	P19	25.52	24.67		11.59	7.10	26.23	5.12	4.06	7.10
0402-014	B	0.920	876	102	P19	27.39	26.45		30.35	15.34	94.68	9.73	7.03	15.34
0410+110	II(G)	0.306				25.15	26.39	F11						
0414+009	B	0.287				24.76	25.30	F11	3.18	2.53	4.68	2.16	1.94	2.53
0414+378	I	0.049	252	230	P19	24.28	24.24							
0419+194	B	0.512	8	1	P19	24.77	23.87		8.39	5.48	17.05	4.13	3.37	5.48
0422+004	B	0.310	1465	1.75	F11	26.61	23.69		78.75	32.88	337.52	18.37	12.12	32.88
0430+05	I	0.033				25.19	24.05	Z95						
0433+29	II(G)	0.218	108.9	13063.54	F11	25.22	27.29							
0449-175	I	0.031				21.58	24.38	Z95						
0453+22	II(G)	0.214	4.1	937.86	F11	23.77	26.13							
0454+844	B	1.340	392	1346.15	F11	27.16	27.69		10.17	6.40	22.03	4.69	3.76	6.40
0502+675	B	0.314	17	4	P19	24.68	24.05		6.69	4.58	12.61	3.55	2.96	4.58

Table 1. (Continued)

Source Name (1)	class (2)	z (3)	S_{core} (mJy) (4)	S_{ext} (mJy) (5)	Ref (6)	$\log L_{\text{core}}$ (W Hz $^{-1}$) (7)	$\log L_{\text{ext}}$ (W Hz $^{-1}$) (8)	Ref (9)	δ_2 ($\alpha_c = 0$) (10)	δ_2 (0.5) (11)	δ_2 (-0.5) (12)	δ_3 ($\alpha_c = 0$) (13)	δ_3 (0.5) (14)	δ_3 (-0.5) (15)
0521-365	B	0.055	3124	5213.24	F11	25.41	25.63		5.39	3.85	9.46	3.08	2.62	3.85
0545-199	I	0.053				23.23	24.00	Z95						
0548-322	B	0.069	80	92.73	F11	24.01	24.07		3.04	2.43	4.40	2.10	1.89	2.43
0605+48	II(G)	0.277	0.5	996.1	F11	23.10	26.40							
0607+710	B	0.267	12	11	P19	24.41	24.38		3.96	3.01	6.27	2.50	2.20	3.01
0620-52	I	0.051	260	946.39	M93	24.25	24.81							
0625-35	I	0.055	600	1650	DM14	24.67	25.11							
0634-205	I	0.055				22.74	24.90	Z95						
0647+250	B	0.203	42	36	P19	24.68	24.61		4.59	3.38	7.62	2.76	2.39	3.38
0648-165	B	0.599	2120	4	P19	27.33	24.60		97.49	39.01	448.70	21.18	13.69	39.01
0651+542	II(G)	0.238	2	963.2	F11	23.57	26.25							
0702+749	II(G)	0.292	9.64	631.90	F11	24.46	26.28							
0704+384	B	0.579	61	260	P19	25.93	26.56		5.28	3.79	9.20	3.03	2.59	3.79
0708+7413	B	0.371	65	151	P19	25.32	25.68		4.69	3.44	7.84	2.80	2.42	3.44
0716+714	B	0.300	2460	88.04	K05	26.77	25.33		31.75	15.90	100.55	10.03	7.21	15.90
0722+30	I	0.019				22.90	22.89	Z95						
0723-008	B	0.128				24.89	25.95	F11	2.40	2.01	3.21	1.79	1.65	2.01
0734+805	II(G)	0.118	7	1271.2	F11	23.44	25.70							
0735+178	B	0.424	1919	59.39	K10	26.98	25.47		36.63	17.83	121.67	11.03	7.83	17.83
0737+746	B	0.315	21	1	P19	24.76	23.43		11.02	6.82	24.53	4.95	3.94	6.82
0738+5451	B	0.720	279	1	P19	26.63	24.18		57.64	25.62	222.65	14.92	10.14	25.62
0742+333	B	0.611	124	1	P19	26.13	24.04		35.92	17.55	118.53	10.89	7.74	17.55
0743+7458	B	0.607	22	11	P19	25.41	25.11		7.65	5.09	15.08	3.88	3.20	5.09
0744+55	I	0.036	105	1596	P19	23.84	25.02							
0749+540	B	0.200	737	133.98	F11	25.89	25.15		12.90	7.74	30.26	5.50	4.31	7.74
0754+100	B	0.266	1087	57.73	F11	26.35	25.07		23.04	12.30	65.56	8.10	6.01	12.30
0759+508	B	0.054	8	10	P19	22.82	22.92		1.68	1.51	2.00	1.41	1.34	1.51
0800+244	I	0.040	4	135	P19	22.48	24.00							
0806+505	B	1.207	12	11	P19	25.83	25.79		7.87	5.21	15.65	3.96	3.25	5.21
0806+524	B	0.138	66	70.8	P19	24.52	24.55		3.98	3.02	6.31	2.51	2.20	3.02
0808+019	B	1.148	424	11.16	F11	27.22	25.64		43.14	20.32	151.29	12.30	8.59	20.32
0810+5619	B	0.510	49	1	P19	25.61	23.92		21.25	11.53	58.86	7.67	5.73	11.53
0812+578	B	0.054	46	18	P19	23.58	23.17		3.39	2.66	5.10	2.26	2.01	2.66
0812+6217	B	0.599	20	18	P19	25.43	25.39		6.52	4.48	12.18	3.49	2.92	4.48
0818-128	B	0.074	270	540	F11	24.59	24.89		3.44	2.69	5.20	2.28	2.03	2.69
0819+525	B	0.599	23	20	P19	25.41	25.35		6.50	4.47	12.14	3.48	2.92	4.47
0820+225	B	0.951				26.42	27.43	F11	5.19	3.73	8.99	3.00	2.56	3.73
0824+294	II(G)	0.458	116.1	636.9	F11	25.97	26.71							
0824+4204	B	0.223	7	40	P19	24.01	24.77		1.92	1.68	2.38	1.54	1.45	1.68
0826+180	B	0.089				23.96	24.50	F11	2.16	1.85	2.80	1.67	1.55	1.85
0828+493	B	0.548				25.90	26.66	F11	4.77	3.49	8.03	2.83	2.44	3.49
0829+046	B	0.174	643	103.90	F11	25.69	24.90		12.13	7.37	27.88	5.28	4.16	7.37
0837-12	B	0.198	160	672	F11	25.28	25.90		3.87	2.95	6.07	2.46	2.17	2.95
0847+548	B	0.367	6	47	P19	24.45	25.34		2.16	1.85	2.79	1.67	1.55	1.85
0850+443	B	0.382	31	46	P19	25.17	25.34		4.96	3.60	8.45	2.91	2.50	3.60
0850+625	B	0.267	224	1	P19	25.68	23.33		34.26	16.90	111.26	10.55	7.53	16.90

Table 1. (Continued)

Source Name (1)	class (2)	z (3)	S_{core} (mJy) (4)	S_{ext} (mJy) (5)	Ref (6)	$\log L_{\text{core}}$ (W Hz $^{-1}$) (7)	$\log L_{\text{ext}}$ (W Hz $^{-1}$) (8)	Ref (9)	δ_2 ($\alpha_c = 0$) (10)	δ_2 (0.5) (11)	δ_2 (-0.5) (12)	δ_3 ($\alpha_c = 0$) (13)	δ_3 (0.5) (14)	δ_3 (-0.5) (15)
0851+203	B	0.306	1719	7	P19	26.67	24.28		56.72	25.29	217.92	14.76	10.05	25.29
0855+082	B	0.455	32	82	P19	25.39	25.80		4.72	3.46	7.91	2.81	2.43	3.46
0905-097	B	0.053				23.69	23.59	F11	2.91	2.35	4.15	2.04	1.84	2.35
0906+041	B	3.200	78	33	P19	27.58	27.21		22.94	12.26	65.18	8.07	5.99	12.26
0908+445	B	0.298	31	126	P19	24.97	25.58		3.36	2.64	5.04	2.24	2.00	2.64
0912+297	B	0.101	222	79.23	F11	24.78	24.33		6.22	4.32	11.44	3.38	2.84	4.32
0915+32	I	0.062				23.12	24.06	Z95						
0915-118	I	0.065				24.51	26.51	Z95						
0917+45	II(G)	0.174	44	1873	F11	24.64	26.27							
0922+3625	B	1.015	167	1	P19	26.77	24.54		53.16	24.01	199.87	14.14	9.68	24.01
0923+750	B	0.638	5	52	P19	24.81	25.83		2.37	2.00	3.16	1.78	1.64	2.00
0925+504	B	0.370	462	615.03	F11	26.16	26.29		8.29	5.43	16.77	4.10	3.35	5.43
0926+2550	B	0.539	113	8	P19	26.04	24.89		18.25	10.21	48.04	6.93	5.26	10.21
0927+352	B	0.435	394	47	F11	26.33	25.41		18.12	10.15	47.59	6.90	5.24	10.15
0927+500	B	0.187	15	7	P19	24.14	23.81		4.22	3.17	6.83	2.61	2.28	3.17
0944+734	I	0.058	131	129	P19	24.06	24.06							
0945+222	B	0.716	48	79	P19	26.00	26.21		7.18	4.84	13.86	3.72	3.09	4.84
0945+664	B	0.850	1407	33	P19	27.57	25.94		52.64	23.82	197.26	14.05	9.63	23.82
0946+003	B	0.585	108	3	P19	26.07	24.51		24.31	12.84	70.41	8.39	6.19	12.84
0950+495	B	0.380	4	1	P19	24.22	23.61		5.25	3.77	9.12	3.02	2.58	3.77
0951+216	B	0.296	33	303	P19	24.94	25.90		2.62	2.16	3.61	1.90	1.73	2.16
0952+226A	B	1.211	17	117	P19	25.92	26.76		4.57	3.37	7.59	2.75	2.38	3.37
0954+65	B	0.368	637	746.53	F11	26.29	26.36		9.15	5.88	19.14	4.37	3.54	5.88
0958+290	II(G)	0.185	34.46	1238.36	F11	24.57	26.13							
0958+294	B	0.558	142	30	P19	26.12	25.45		13.84	8.18	33.23	5.76	4.49	8.18
0958+426A	B	0.664	23	37	P19	25.51	25.71		5.71	4.03	10.21	3.20	2.71	4.03
1003+328	B	1.026	58	173	P19	26.43	26.90		7.44	4.98	14.53	3.81	3.15	4.98
1003+351	II(G)	0.101	900	772	F11	25.40	25.33							
1009+427	B	0.365	29	17	P19	25.09	24.86		6.26	4.34	11.53	3.40	2.85	4.34
1011+446	B	0.796	7	15	P19	25.33	25.66		4.83	3.53	8.17	2.86	2.46	3.53
1011+496	B	0.212				24.91	24.98	F11	4.69	3.44	7.84	2.80	2.42	3.44
1015+383	B	0.387	16	101	P19	24.92	25.72		2.89	2.34	4.12	2.03	1.83	2.34
1020+493	B	0.390	12	52	P19	24.73	25.37		2.95	2.37	4.22	2.06	1.85	2.37
1027+555A	B	0.435	7	73	P19	24.72	25.74		2.27	1.93	2.98	1.73	1.60	1.93
1028+511	B	0.360	23	11	P19	24.93	24.61		6.14	4.27	11.23	3.35	2.82	4.27
1030+585	II(G)	0.428	1.38	837.37	NED	23.99	26.78							
1034+5727	B	0.830	89	37	P19	26.13	25.75		11.44	7.03	25.78	5.08	4.03	7.03
1040+31	I	0.036				23.48	24.14	Z95						
1044+549	B	0.540	4	2	P19	24.57	24.27		5.08	3.67	8.74	2.96	2.53	3.67
1055+0519	B	0.890	179	25	P19	26.62	25.76		19.85	10.92	53.75	7.33	5.52	10.92
1055+567	B	0.143	178	69	P19	24.98	24.57		6.68	4.57	12.58	3.55	2.96	4.57
1101+384	B	0.030	520	156.65	F11	24.09	23.57		4.68	3.44	7.83	2.80	2.42	3.44
1101+411	B	0.035	13	8	P19	22.61	22.40		1.86	1.64	2.28	1.51	1.42	1.64
1106+244	B	0.482	18	1	P19	25.16	23.90		12.81	7.69	29.96	5.47	4.29	7.69
1116+227	B	0.422	104	34	P19	25.67	25.18		9.81	6.21	20.99	4.58	3.69	6.21
1118+424	B	0.124	19	11	P19	23.87	23.64		3.49	2.72	5.28	2.30	2.04	2.72

Table 1. (Continued)

Source Name (1)	class (2)	z (3)	S_{core} (mJy) (4)	S_{ext} (mJy) (5)	Ref (6)	$\log L_{\text{core}}$ (W Hz $^{-1}$) (7)	$\log L_{\text{ext}}$ (W Hz $^{-1}$) (8)	Ref (9)	δ_2 ($\alpha_c = 0$) (10)	δ_2 (0.5) (11)	δ_2 (-0.5) (12)	δ_3 ($\alpha_c = 0$) (13)	δ_3 (0.5) (14)	δ_3 (-0.5) (15)
1122+39	I	0.007				21.06	23.16	Z95						
1133+704	B	0.045	131	220.48	F11	23.83	24.06		2.50	2.08	3.40	1.84	1.69	2.08
1142+198	I	0.022	250	2107.56	F11	23.52	24.44							
1144+352	B	0.063	537	126	F11	24.74	24.12		6.90	4.69	13.14	3.63	3.02	4.69
1144-379	B	1.048	2182	18	P19	27.66	25.58		74.60	31.49	314.06	17.72	11.75	31.49
1145+1936	I	0.021				23.30	24.36	B11						
1147+245	B	0.200	664	20	F11	25.86	24.33		21.41	11.60	59.46	7.71	5.76	11.60
1148+592	B	0.118	95	36	P19	24.55	24.13		5.47	3.89	9.63	3.10	2.64	3.89
1150+449A	B	0.599	9	5	P19	25.00	24.74		6.08	4.24	11.10	3.33	2.81	4.24
1151+6039	B	1.120	75	1	P19	26.69	24.82		40.68	19.39	139.89	11.83	8.31	19.39
1154+435	B	0.230	93	13	P19	25.19	24.33		9.94	6.28	21.37	4.62	3.71	6.28
1202+492	B	0.452	40	71	P19	25.47	25.72		5.45	3.88	9.58	3.10	2.63	3.88
1203+238	B	0.599	8	30	P19	24.95	25.52		3.41	2.67	5.13	2.27	2.02	2.67
1203+645	II(G)	0.372	730	579	F11	26.56	26.46							
1208+322	B	0.389	7	149	P19	24.56	25.89		1.71	1.53	2.04	1.43	1.36	1.53
1210+121	B	0.369	170	81.97	F11	25.91	25.59		9.83	6.22	21.05	4.59	3.69	6.22
1215+303	B	0.130	355	157.77	F11	25.21	24.85		7.17	4.83	13.82	3.72	3.08	4.83
1216+06	I	0.006				22.68	23.98	Z95						
1217+348	B	0.643	258	94	P19	26.43	25.99		13.71	8.12	32.81	5.73	4.46	8.12
1218+285	B	0.102	1118	10.52	P19	25.53	23.50		25.63	13.40	75.58	8.69	6.38	13.40
1218+460	B	0.525	30	37	P19	25.37	25.46		5.78	4.07	10.36	3.22	2.72	4.07
1220+337C	B	0.599	459	383	P19	26.81	26.73		12.98	7.78	30.52	5.52	4.33	7.78
1220+373	B	0.491	15	138	P19	25.17	26.13		2.92	2.36	4.17	2.04	1.84	2.36
1221+245	B	0.218	179	25	P19	25.37	24.52		10.86	6.74	24.06	4.91	3.91	6.74
1221+809	B	0.369	447	71	F11	26.25	25.46		16.04	9.21	40.45	6.36	4.88	9.21
1222+13	I	0.003				21.72	23.23	F11						
1222+488	B	0.647	20	18	P19	25.50	25.45		6.73	4.60	12.70	3.56	2.97	4.60
1227+255	B	0.135	351	1	P19	25.26	22.71		31.76	15.90	100.57	10.03	7.21	15.90
1228+12	I	0.004	3097	68469	DM14	23.34	24.69							
1229.2+6430	B	0.163	42.49	3.48	F11	24.48	23.39		8.25	5.41	16.67	4.08	3.34	5.41
1229+290	B	0.236	60	54	P19	25.00	24.95		5.28	3.79	9.21	3.03	2.59	3.79
1229+405	B	0.638	52	57	P19	25.98	26.02		8.03	5.29	16.08	4.01	3.29	5.29
1235+632	B	0.297	22	21	P19	24.74	24.72		4.60	3.39	7.64	2.76	2.39	3.39
1238+414	B	0.499	10	19	P19	24.84	25.11		3.93	2.99	6.21	2.49	2.19	2.99
1239+069	B	0.150	10	1	P19	23.80	22.80		5.59	3.96	9.91	3.15	2.67	3.96
1243+4402	B	1.152	43	5	P19	26.33	25.40		18.25	10.21	48.05	6.93	5.26	10.21
1246+586	B	0.847	278	136	F11	26.64	26.33		13.94	8.23	33.56	5.79	4.51	8.23
1247+443	B	1.812	12	4	P19	25.90	25.42		10.88	6.75	24.11	4.91	3.91	6.75
1250+532	B	0.369	346	50	F11	26.34	25.50		17.19	9.73	44.37	6.66	5.08	9.73
1251+278	II(G)	0.086				22.99	25.38	F11						
1251-12	I	0.014				22.87	24.30	Z95						
1254+476	II(G)	0.996	1.6	1352.96	F11	24.92	27.85							
1255+244	B	0.141	7	1	P19	23.60	22.75		4.57	3.37	7.59	2.75	2.38	3.37
1259+2757	I	0.024				21.10	22.99	B11						
1259+4112	B	0.649	19	14	P19	25.34	25.21		6.60	4.53	12.38	3.52	2.94	4.53
1302+715	B	0.599	31	1	P19	25.51	24.02		17.80	10.01	46.47	6.82	5.18	10.01

Table 1. (Continued)

Source Name (1)	class (2)	z (3)	S_{core} (mJy) (4)	S_{ext} (mJy) (5)	Ref (6)	$\log L_{\text{core}}$ (W Hz $^{-1}$) (7)	$\log L_{\text{ext}}$ (W Hz $^{-1}$) (8)	Ref (9)	δ_2 ($\alpha_c = 0$) (10)	δ_2 (0.5) (11)	δ_2 (-0.5) (12)	δ_3 ($\alpha_c = 0$) (13)	δ_3 (0.5) (14)	δ_3 (-0.5) (15)
1308+27	II(G)	0.240	2.79	472.09	F11	23.74	25.97							
1309-216	B	1.491	140	45	F11	27.20	26.71		20.66	11.27	56.69	7.53	5.64	11.27
1310+560	B	0.975	235	33	P19	26.99	26.14		23.74	12.60	68.22	8.26	6.11	12.60
1312+240	B	2.145	101	31	P19	27.26	26.74		21.51	11.65	59.83	7.74	5.77	11.65
1318-43	I	0.011				23.48	24.18	Z95						
1319+428	II(G)	0.079				22.69	25.27	F11						
1322+36	I	0.018				23.29	23.49	Z95						
1324+478	B	0.683	15	30	P19	25.29	25.59		4.83	3.52	8.16	2.86	2.46	3.52
1328+506	B	0.599	19	3	P19	25.24	24.44		9.83	6.22	21.05	4.59	3.69	6.22
1338+3851	I	0.246				24.70	26.19	B11						
1339+554	B	0.207	30	4	P19	24.54	23.66		7.37	4.94	14.33	3.79	3.13	4.94
1343-60	I	0.013	2730	3850	DM14	24.09	24.24							
1345+735	B	0.290	17	372	P19	24.67	26.01		1.79	1.59	2.17	1.47	1.39	1.59
1346+26	I	0.063				23.95	24.91	Z95						
1350+4922	B	0.397	63	61	P19	25.38	25.36		6.21	4.31	11.43	3.38	2.84	4.31
1356+393	B	0.800	63	31	P19	26.30	25.99		11.81	7.21	26.90	5.19	4.10	7.21
1400+162	B	0.244	233	311.19	F11	25.62	25.75		6.36	4.39	11.79	3.43	2.88	4.39
1402+042	B	0.344	21	12	P19	24.86	24.62		5.64	3.99	10.04	3.17	2.69	3.99
1404+286	B	0.077	991	1909	P19	25.11	25.40		4.48	3.32	7.38	2.72	2.36	3.32
1407+595	B	0.496	17	3	P19	25.09	24.34		8.88	5.74	18.39	4.29	3.48	5.74
1409+524	II(G)	0.464	10	7364	NED	24.93	27.80							
1413+135	B	0.247	1080	4.091	K10	26.27	23.85		47.86	22.08	173.76	13.18	9.12	22.08
1414+110	I	0.025	56	1649.57	F11	22.96	24.43							
1414+375	B	0.920	41	4	P19	26.17	25.16		17.78	10.00	46.39	6.81	5.18	10.00
1418+546	B	0.153	1058	19.82	F11	25.80	24.08		23.98	12.70	69.14	8.31	6.14	12.70
1420+198	II(G)	0.270	6.2	894.32	F11	24.16	26.32							
1421+582	B	0.635	6	89	P19	24.51	25.68		1.85	1.64	2.27	1.51	1.42	1.64
1422+026	I	0.037	662	1868	P19	24.60	25.05							
1424+240	B	0.160	250	60	P19	25.23	24.61		8.68	5.64	17.85	4.23	3.44	5.64
1426+340	B	1.553	23	5	P19	26.32	25.65		15.08	8.76	37.26	6.10	4.71	8.76
1426+428	B	0.129	19.1	2.1	P19	23.91	22.95		5.75	4.05	10.30	3.21	2.72	4.05
1435+174A	B	0.599	355	174	P19	26.60	26.29		13.65	8.09	32.61	5.71	4.45	8.09
1437+397	B	0.344	38	24	P19	25.06	24.86		6.03	4.21	10.98	3.31	2.79	4.21
1440+122	B	0.163	17.2	1.3	P19	24.09	22.97		6.99	4.74	13.37	3.66	3.04	4.74
1440+356	B	0.079	1	13	P19	22.17	23.28		0.62	0.68	0.53	0.73	0.76	0.68
1441+522	II(G)	0.722	104	938.4	F11	24.74	25.69							
1441+536	B	2.454	17	1	P19	26.77	25.54		27.45	14.15	82.80	9.10	6.64	14.15
1443+634	B	0.298	8	7	P19	24.30	24.25		3.81	2.91	5.94	2.44	2.15	2.91
1446+3620	B	1.565	29	1	P19	26.85	25.39		33.28	16.51	107.07	10.35	7.41	16.51
1447+771	II(G)	1.132	6	454	F11	25.67	27.55							
1448+634	I	0.042				22.57	24.73	F11						
1449+537	B	0.432	6	16	P19	24.57	25.00		3.14	2.50	4.60	2.14	1.92	2.50
1452+516	B	1.083	80	53	P19	26.51	26.33		11.99	7.29	27.44	5.24	4.13	7.29
1454+510	B	0.599	212	20	P19	26.32	25.30		19.27	10.67	51.68	7.19	5.42	10.67
1458+224	B	0.235	60	25	P19	24.88	24.50		6.22	4.32	11.45	3.38	2.84	4.32
1459+551	B	0.339	18	56	P19	24.85	25.34		3.44	2.68	5.18	2.28	2.02	2.68

Table 1. (Continued)

Source Name	class	z	S_{core} (mJy)	S_{ext} (mJy)	Ref	$\log L_{\text{core}}$ (W Hz $^{-1}$)	$\log L_{\text{ext}}$ (W Hz $^{-1}$)	Ref	δ_2 ($\alpha_c = 0$)	δ_2 0.5	δ_2 -0.5)	δ_3 ($\alpha_c = 0$)	δ_3 0.5	δ_3 -0.5)
(1)	(2)	(3)	(4)	(5)	(6)	(7)	(8)	(9)	(10)	(11)	(12)	(13)	(14)	(15)
1501+481	B	0.345	10	46	P19	24.63	25.29		2.75	2.25	3.85	1.96	1.78	2.25
1504+2600	I	0.054				23.70	24.87	B11						
1508+3138	B	0.672	83	51	P19	25.95	25.73		9.33	5.97	19.65	4.43	3.58	5.97
1508+425	B	0.488	19	92	P19	25.22	25.91		3.62	2.80	5.55	2.36	2.08	2.80
1508+561	B	1.680	28	16	P19	26.22	25.98		10.88	6.75	24.10	4.91	3.91	6.75
1508+574	B	0.817	10	36	P19	25.26	25.82		4.02	3.04	6.39	2.53	2.21	3.04
1514+07	I	0.035				24.50	25.28	Z95						
1514+197	B	1.070	255	2.62	F11	26.81	24.82		46.38	21.53	166.66	12.91	8.96	21.53
1514-241	B	0.049	2562	3.02	F11	25.20	22.27		39.97	19.11	136.64	11.69	8.23	19.11
1516+0701	I	0.034				23.90	24.23	B11						
1516+4843	B	0.576	5	29	P19	24.80	25.56		2.79	2.27	3.93	1.98	1.80	2.27
1517+656	B	0.702	19	19	P19	25.33	25.33		6.01	4.20	10.93	3.31	2.79	4.20
1519-273	B	1.294	2290	10	P19	28.00	25.64		105.52	41.56	498.63	22.33	14.33	41.56
1525+29	I	0.065				22.66	24.07	Z95						
1529+5153	B	0.975	21	8	P19	25.70	25.28		9.51	6.06	20.16	4.49	3.62	6.06
1530+190	B	0.307	17	11	P19	24.62	24.43		4.84	3.53	8.19	2.86	2.46	3.53
1532+595	B	0.599	13	25	P19	25.31	25.59		4.93	3.58	8.39	2.90	2.49	3.58
1533+342	B	0.811	33	1	P19	25.86	24.34		21.41	11.60	59.45	7.71	5.76	11.60
1533+535	B	0.890	43	1	P19	25.80	24.17		22.50	12.07	63.54	7.97	5.93	12.07
1534+0147	B	0.312	25	9	P19	24.96	24.52		6.76	4.61	12.78	3.58	2.98	4.61
1534+656	B	0.539	6	50	P19	24.82	25.74		2.54	2.11	3.46	1.86	1.70	2.11
1538+149	B	0.605	1337	125.89	F11	27.17	26.15		29.11	14.83	89.55	9.46	6.86	14.83
1552.1+2020	B	0.222	33.09	10.09	F11	24.68	24.16		6.19	4.30	11.36	3.37	2.83	4.30
1553+113	B	0.360	95	29.38	P19	25.51	25.00		9.21	5.91	19.31	4.39	3.56	5.91
1553-228	I	0.065	126	42	P19	24.20	23.72							
1600+309	B	1.091	20	4	P19	26.07	25.37		13.72	8.13	32.84	5.73	4.47	8.13
1604+1353	B	0.294	32	21	P19	24.89	24.70		5.48	3.90	9.67	3.11	2.64	3.90
1615+351	I	0.030	32	68	F11	23.20	23.52							
1615+412	B	0.267	81	43	P19	25.17	24.90		6.70	4.58	12.63	3.55	2.96	4.58
1618+063	B	0.435	17	14	P19	24.99	24.90		5.40	3.85	9.47	3.08	2.62	3.85
1619+378	B	1.272	155	46	P19	27.18	26.65		20.88	11.37	57.50	7.58	5.68	11.37
1620+103	B	0.369	85	55.83	F11	25.62	25.44		7.81	5.18	15.50	3.94	3.24	5.18
1621+38	I	0.031				23.31	23.74	Z95						
1622+375	B	0.200	14	17	P19	24.20	24.28		3.29	2.59	4.89	2.21	1.97	2.59
1622-253	B	0.786	179	25	P19	26.54	25.69		19.11	10.59	51.11	7.15	5.40	10.59
1625+318	B	0.732	38	38	P19	25.89	25.89		7.89	5.22	15.71	3.96	3.26	5.22
1626+352	B	0.497	14	5	P19	25.02	24.58		7.00	4.74	13.38	3.66	3.04	4.74
1626+396	I	0.030				23.16	24.49	F11						
1626+518	I	0.055	96	78	P19	24.05	23.96							
1629+120	B	1.795	359	505	P19	27.72	27.87		17.30	9.78	44.74	6.69	5.10	9.78
1635+185B	B	0.599	124	17	P19	26.14	25.28		15.83	9.11	39.75	6.30	4.85	9.11
1636+8240	I	0.025	380	130	DM14	23.76	23.30							
1640+396	B	0.539	47	5	P19	25.59	24.62		13.10	7.83	30.87	5.56	4.35	7.83
1643+1715	I	0.162				25.10	25.94	B11						
1651+0459	I	0.154				23.90	26.80	B11						
1652+151	B	0.290	67	30	P19	25.24	24.89		7.26	4.88	14.05	3.75	3.10	4.88

Table 1. (Continued)

Source Name (1)	class (2)	z (3)	S_{core} (mJy) (4)	S_{ext} (mJy) (5)	Ref (6)	$\log L_{\text{core}}$ (W Hz $^{-1}$) (7)	$\log L_{\text{ext}}$ (W Hz $^{-1}$) (8)	Ref (9)	δ_2 ($\alpha_c = 0$) (10)	δ_2 (0.5) (11)	δ_2 (-0.5) (12)	δ_3 ($\alpha_c = 0$) (13)	δ_3 (0.5) (14)	δ_3 (-0.5) (15)
1652+398	B	0.034	1376	63.85	F11	24.59	23.26		10.24	6.43	22.24	4.72	3.78	6.43
1658+471	II(G)	0.205	16.7	1296.52	F11	24.33	26.22							
1659+389	B	1.113	50	11	P19	26.58	25.92		17.06	9.67	43.93	6.63	5.06	9.67
1700+518	B	0.292	2	4	P19	23.72	24.02		2.26	1.92	2.96	1.72	1.59	1.92
1702+298	B	1.927	258	306	P19	27.75	27.82		18.44	10.30	48.72	6.98	5.29	10.30
1705+7142	B	0.350	17	26	P19	24.75	24.93		4.01	3.04	6.37	2.52	2.21	3.04
1706+36	B	0.918	15	12	P19	25.53	25.43		7.06	4.77	13.54	3.68	3.05	4.77
1707+344	I	0.081	5	196	P19	22.95	24.54							
1713+504	B	1.090	21	39	P19	25.99	26.26		6.91	4.70	13.17	3.63	3.02	4.70
1715+574A	B	0.599	14	21	P19	25.19	25.37		5.00	3.63	8.56	2.93	2.51	3.63
1717+178	B	0.137	661	8.043	F11	25.52	23.61		23.69	12.58	68.05	8.25	6.10	12.58
1731+325	B	0.375	37	187	P19	25.19	25.89		3.51	2.73	5.34	2.31	2.05	2.73
1733+453	B	0.317	13	6	P19	24.60	24.27		5.30	3.79	9.23	3.04	2.59	3.79
1738+1944	B	0.599	143	69	P19	26.24	25.92		11.54	7.08	26.09	5.11	4.05	7.08
1738+476	B	0.950	848	1	F11	27.35	24.42		113.08	43.93	546.83	23.38	14.91	43.93
1747+433	B	0.215	295	72	F11	25.55	24.94		10.07	6.35	21.75	4.66	3.74	6.35
1749+701	B	0.770	1754	89.16	F11	27.59	26.30		42.60	20.12	148.79	12.20	8.53	20.12
1750+374	B	0.599	28	5	P19	25.34	24.59		9.97	6.29	21.45	4.63	3.72	6.29
1752+3212	B	0.599	35	7	P19	25.62	24.92		11.01	6.82	24.50	4.95	3.94	6.82
1756+553	B	2.085	10	4	P19	26.12	25.72		11.51	7.06	25.98	5.10	4.04	7.06
1757+703	B	0.407	11	1	P19	24.73	23.69		9.04	5.82	18.84	4.34	3.52	5.82
1800+664	B	0.026	5	2	P19	21.96	21.56		1.53	1.41	1.77	1.33	1.28	1.41
1807+698	B	0.051	1520	430	F11	24.99	24.44		7.36	4.94	14.32	3.78	3.13	4.94
1811+442	B	0.350	6	22	P19	24.31	24.88		2.52	2.10	3.43	1.85	1.70	2.10
1831+401	B	0.599	23	3	P19	25.62	24.73		12.47	7.53	28.93	5.38	4.23	7.53
1831+559	B	0.599	13	5	P19	25.28	24.86		7.74	5.14	15.32	3.91	3.22	5.14
1832+315	B	0.599	339	698	P19	26.65	26.96		9.24	5.92	19.39	4.40	3.56	5.92
1832+474	II(G)	0.161	7.8	1445.28	F11	23.77	26.04							
1833+326	II(G)	0.058	160	1600	F11	24.14	25.14							
1836+171	I	0.017	17	2907.22	F11	22.06	24.29							
1839-48	I	0.112				24.98	25.87	Z95						
1841+317	B	0.448	42	100	P19	25.40	25.78		4.84	3.53	8.19	2.86	2.46	3.53
1842+455	II(G)	0.092				23.76	25.73	F11						
1848+427	B	0.599	8	16	P19	24.89	25.19		3.98	3.02	6.31	2.51	2.20	3.02
1853+671	B	0.212	12	1	P19	24.15	23.07		6.99	4.74	13.36	3.65	3.04	4.74
1914-194	B	0.137	293	124	P19	25.16	24.78		7.10	4.80	13.64	3.69	3.06	4.80
1915+3419	B	0.599	34	1	P19	25.59	24.06		18.97	10.53	50.60	7.11	5.37	10.53
1926+611	B	0.369	825	1	F11	26.49	23.57		73.88	31.25	310.03	17.61	11.69	31.25
1939+605	II(G)	0.201	28.54	1141.64	F11	24.56	26.16							
1954-55	I	0.060				23.91	25.60	Z95						
1957+4035	I	0.056	277	276	P19	24.34	24.34							
2003+454	B	0.599	557	110	P19	26.81	26.11		19.73	10.86	53.30	7.30	5.50	10.86
2005-489	B	0.071	454	736	P19	24.75	24.96		3.95	3.00	6.25	2.50	2.19	3.00
2007+777	B	0.342	823	50.28	PS93	26.36	25.15		22.30	11.98	62.76	7.92	5.89	11.98
2010+723	B	0.369	1338	1	F11	26.72	23.59		94.84	38.16	432.51	20.80	13.48	38.16
2013-308	I	0.089				23.03	24.51	Z95						

Table 1. (Continued)

Source Name (1)	class (2)	z (3)	S_{core} (mJy) (4)	S_{ext} (mJy) (5)	Ref (6)	$\log L_{\text{core}}$ (W Hz $^{-1}$) (7)	$\log L_{\text{ext}}$ (W Hz $^{-1}$) (8)	Ref (9)	δ_2 ($\alpha_c = 0$) (10)	δ_2 (0.5) (11)	δ_2 (-0.5) (12)	δ_3 ($\alpha_c = 0$) (13)	δ_3 (0.5) (14)	δ_3 (-0.5) (15)
2020+6409	B	0.599	125	20	P19	26.10	25.30		14.86	8.66	36.53	6.04	4.67	8.66
2021+317	B	0.599	3060	58	P19	27.50	25.78		54.31	24.43	205.66	14.34	9.80	24.43
2022+542	B	0.599	991	100	P19	27.04	26.05		26.77	13.87	80.09	8.95	6.54	13.87
2023+76	B	0.594	425	349	P19	26.46	26.38		11.02	6.82	24.51	4.95	3.94	6.82
2028+1925	B	0.599	40	2	P19	25.65	24.35		16.78	9.55	42.96	6.55	5.01	9.55
2029+121	B	1.215	1006	222	P19	27.51	26.85		26.71	13.85	79.85	8.94	6.54	13.85
2030+547	B	1.262	943	54	P19	27.67	26.42		42.67	20.14	149.11	12.21	8.54	20.14
2032+117	B	0.607	102	78	P19	26.13	26.02		9.58	6.10	20.36	4.51	3.64	6.10
2048+0701	I	0.127				23.80	25.49	B11						
2052+0003	B	0.151	44	21	P19	24.40	24.08		4.76	3.49	8.02	2.83	2.44	3.49
2053-201	I	0.156				23.79	25.47	Z95						
2058-282	I	0.040	63	1937	P19	23.37	24.85							
2104+763	II(G)	0.572	0.89	752.71	NED	24.10	27.02							
2104-256	I	0.039				22.94	24.48	Z95						
2116+203	B	1.680	110	101	P19	27.01	26.97		13.90	8.21	33.42	5.78	4.50	8.21
2116+26	I	0.016				22.73	22.69	Z95						
2124+505	I	0.020	534	424	P19	23.90	23.80							
2131-021	B	1.285				27.60	25.60	F11	68.55	29.43	280.54	16.75	11.20	29.43
2136-251	B	0.940	179	150	P19	26.94	26.87		13.82	8.17	33.16	5.76	4.48	8.17
2141+279	II(G)	0.215	17.9	803.74	F11	24.41	26.06							
2143.4+0704	B	0.237	44.63	23.15	F11	24.85	24.56		5.76	4.06	10.32	3.21	2.72	4.06
2144+147	B	0.599	23	1	P19	25.54	24.18		16.51	9.42	42.03	6.48	4.96	9.42
2149+17	B	0.871	648	372	P19	27.14	26.90		16.96	9.63	43.59	6.60	5.04	9.63
2152-69	I	0.027				24.11	25.56	Z95						
2153+377	II(G)	0.290	9	2565.2	F11	24.44	26.89							
2155-304	B	0.117	350	218.23	F11	25.08	24.87		6.10	4.25	11.15	3.34	2.81	4.25
2158-206	B	0.370	87	23	P19	25.69	25.11		10.51	6.56	23.01	4.80	3.83	6.56
2200+420	B	0.069	1990	11.03	K10	25.36	23.11		27.60	14.22	83.42	9.13	6.66	14.22
2201+044	B	0.028				23.41	24.00	F11	1.60	1.46	1.88	1.37	1.31	1.46
2208+457	B	0.599	39	1	P19	25.64	24.05		20.19	11.07	54.98	7.42	5.57	11.07
2209+236	B	1.125	430	1	P19	27.45	24.82		97.55	39.03	449.04	21.19	13.70	39.03
2213+287	B	0.229	103	74	P19	25.25	25.11		6.38	4.40	11.83	3.44	2.88	4.40
2214+1350	I	0.026				21.50	24.10	B11						
2214+241	B	0.505	420	265	P19	26.44	26.24		11.77	7.19	26.77	5.17	4.09	7.19
2223-052	B	1.404				28.70	27.20	F11	83.56	34.48	365.31	19.11	12.54	34.48
2225+692	B	0.599	27	67	P19	25.60	26.00		5.27	3.78	9.17	3.03	2.58	3.78
2231+3921	I	0.018				22.40	23.57	B11						
2243+394	II(G)	0.081				24.23	25.47	F11						
2251+006	B	0.939	244	175	P19	26.88	26.74		14.03	8.27	33.82	5.82	4.52	8.27
2251+244	B	2.328	134	666	P19	27.50	28.19		10.77	6.70	23.79	4.88	3.89	6.70
2254+074	B	0.190	454	14.54	F11	25.64	24.15		18.96	10.53	50.55	7.11	5.37	10.53
2309+184	II(G)	0.428	7	744.4	F11	24.72	26.75							
2313+147	B	0.163	26	1	P19	24.27	22.86		9.29	5.95	19.53	4.42	3.57	5.95
2315+115	B	0.567	13	16	P19	25.14	25.23		5.16	3.71	8.91	2.98	2.55	3.71
2318+235	II(G)	0.268	21	369	P19	24.72	25.96							
2320+0813	I	0.011				21.60	22.77	B11						

Table 1. (Continued)

Source Name (1)	class (2)	z (3)	S_{core} (mJy) (4)	S_{ext} (mJy) (5)	Ref (6)	$\log L_{\text{core}}$ (W Hz $^{-1}$) (7)	$\log L_{\text{ext}}$ (W Hz $^{-1}$) (8)	Ref (9)	δ_2 ($\alpha_c = 0$) (10)	δ_2 (0.5) (11)	δ_2 (-0.5) (12)	δ_3 ($\alpha_c = 0$) (13)	δ_3 (0.5) (14)	δ_3 (-0.5) (15)
2320+343	B	0.098	30	48	P19	23.86	24.07		2.58	2.13	3.54	1.88	1.72	2.13
2320+417	B	0.152	7	39	P19	23.64	24.39		1.62	1.47	1.90	1.38	1.32	1.47
2322-123	I	0.082	12	380	P19	23.33	24.83							
2326+174	B	0.213	18	8	P19	24.33	23.98		4.70	3.45	7.87	2.81	2.42	3.45
2329+3433	B	0.599	25	3	P19	25.56	24.64		12.42	7.50	28.75	5.36	4.22	7.50
2335+267	I	0.030				23.37	24.84	F11						
2335+358	B	2.280	29	96	P19	26.69	27.21		8.21	5.39	16.57	4.07	3.33	5.39
2338+2701	I	0.030				23.70	24.54	B11						
2343-151	B	0.224	8	1	P19	24.04	23.14		5.89	4.13	10.64	3.26	2.75	4.13
2347+1924	B	0.515	3	1	P19	24.38	23.91		5.24	3.76	9.10	3.02	2.58	3.76
2354-113	B	0.949	12	276	P19	25.52	26.88		2.66	2.19	3.68	1.92	1.75	2.19